

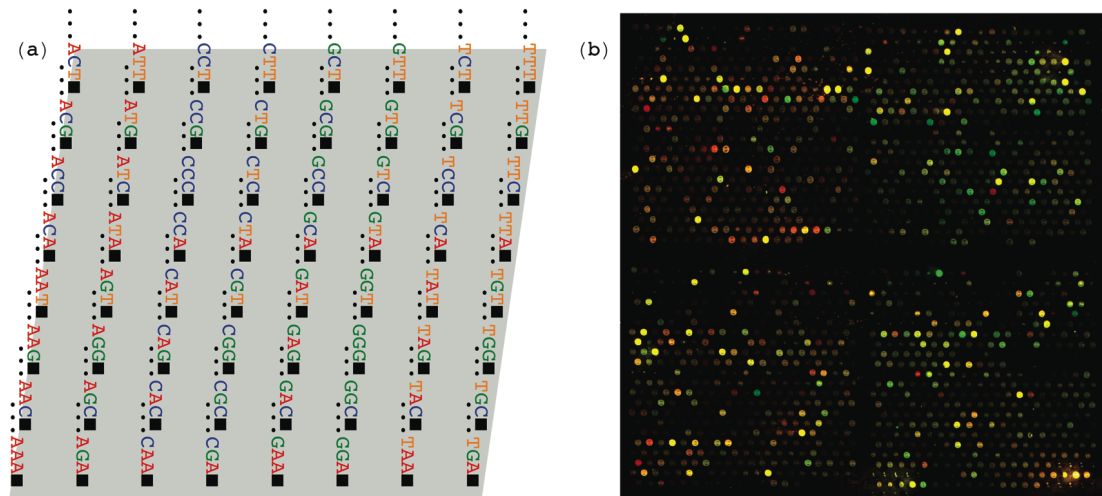
**Cancer Diagnostics and Prognostics from
Comparative Spectral Decompositions of
Patient-Matched Genomic Profiles**

Orly Alter

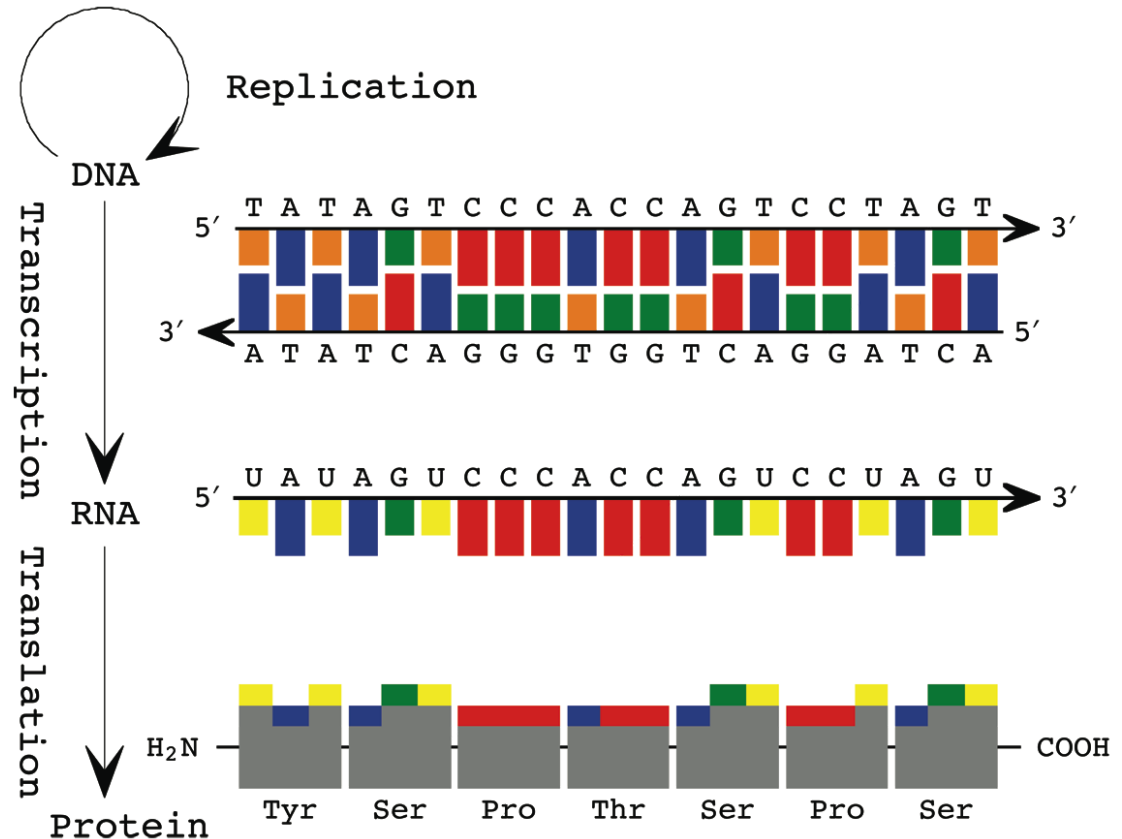
**Departments of Bioengineering and Human Genetics,
Scientific Computing and Imaging Institute and
Huntsman Cancer Institute,
University of Utah, and the
Utah Science, Technology, and Research (USTAR) Initiative**

**orly@sci.utah.edu
<http://alterlab.org/>**

High-Throughput Biotechnologies Record Global Signals



DNA microarrays, e.g., rely on hybridization to record the complete genomic signals that guide the progression of cellular processes, such as abundance levels of DNA, RNA, and DNA- and RNA-bound proteins on a genomic scale.



A groundbreaking look at the nature of quantum mechanics

With new technologies permitting the observation and manipulation of single quantum systems, the quantum theory of measurement is fast becoming a subject of experimental investigation in laboratories worldwide. This original new work addresses open fundamental questions in quantum mechanics in light of these experimental developments.

Using a novel analytical approach developed by the authors, *Quantum Measurement of a Single System* provides answers to three long-standing questions that have been debated by such thinkers as Bohr, Einstein, Heisenberg, and Schrödinger. It establishes the quantum theoretical limits to information obtained in the measurement of a single system on the quantum wavefunction of the system, the time evolution of the quantum observables associated with the system, and the classical potentials or forces which shape this time evolution. The technological relevance of the theory is also demonstrated through examples from atomic physics, quantum optics, and mesoscopic physics.

Suitable for professionals, students, or readers with a general interest in quantum mechanics, the book features recent formulations as well as humorous illustrations of the basic concepts of quantum measurement. Researchers in physics and engineering will find *Quantum Measurement of a Single System* a timely guide to one of the most stimulating fields of science today.

ORLY ALTER, PhD, is currently a postdoctoral fellow in the Department of Genetics at Stanford University. **YOSHIHISA YAMAMOTO, PhD**, is a professor in the Departments of Applied Physics and Electrical Engineering at Stanford University. He is currently the director of the ICORP Quantum Entanglement Project of the Japanese Science and Technology (JST) Corporation. While they collaborated on the research presented in this book, Yamamoto was the director of the ERATO Quantum Fluctuation Project of JST, and Alter was a doctoral student at the Department of Applied Physics at Stanford. She was selected as a finalist for the American Physical Society Award for Outstanding Doctoral Thesis Research in Atomic, Molecular or Optical Physics for 1998 for this work.

Cover Illustration: David B. Oberman

WILEY-INTERSCIENCE

John Wiley & Sons, Inc.
Scientific, Technical, and Medical Division
605 Third Avenue, New York, N.Y. 10158-0012
New York • Chichester • Weinheim
Brisbane • Singapore • Toronto



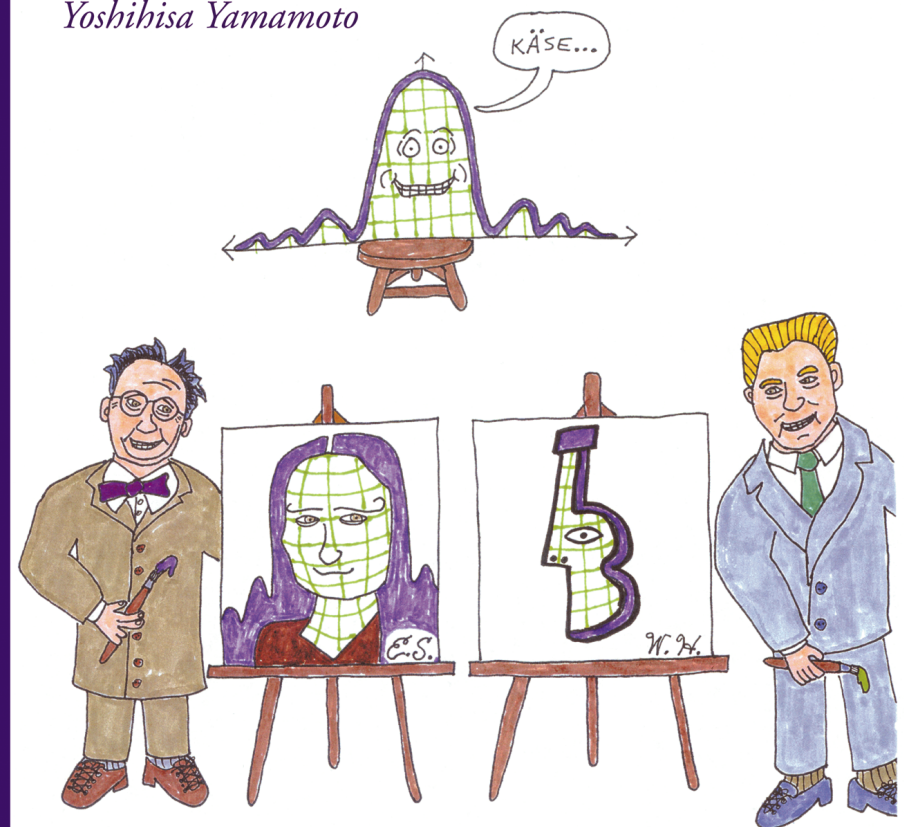
ALTER
YAMAMOTO

Quantum Measurement of a Single System

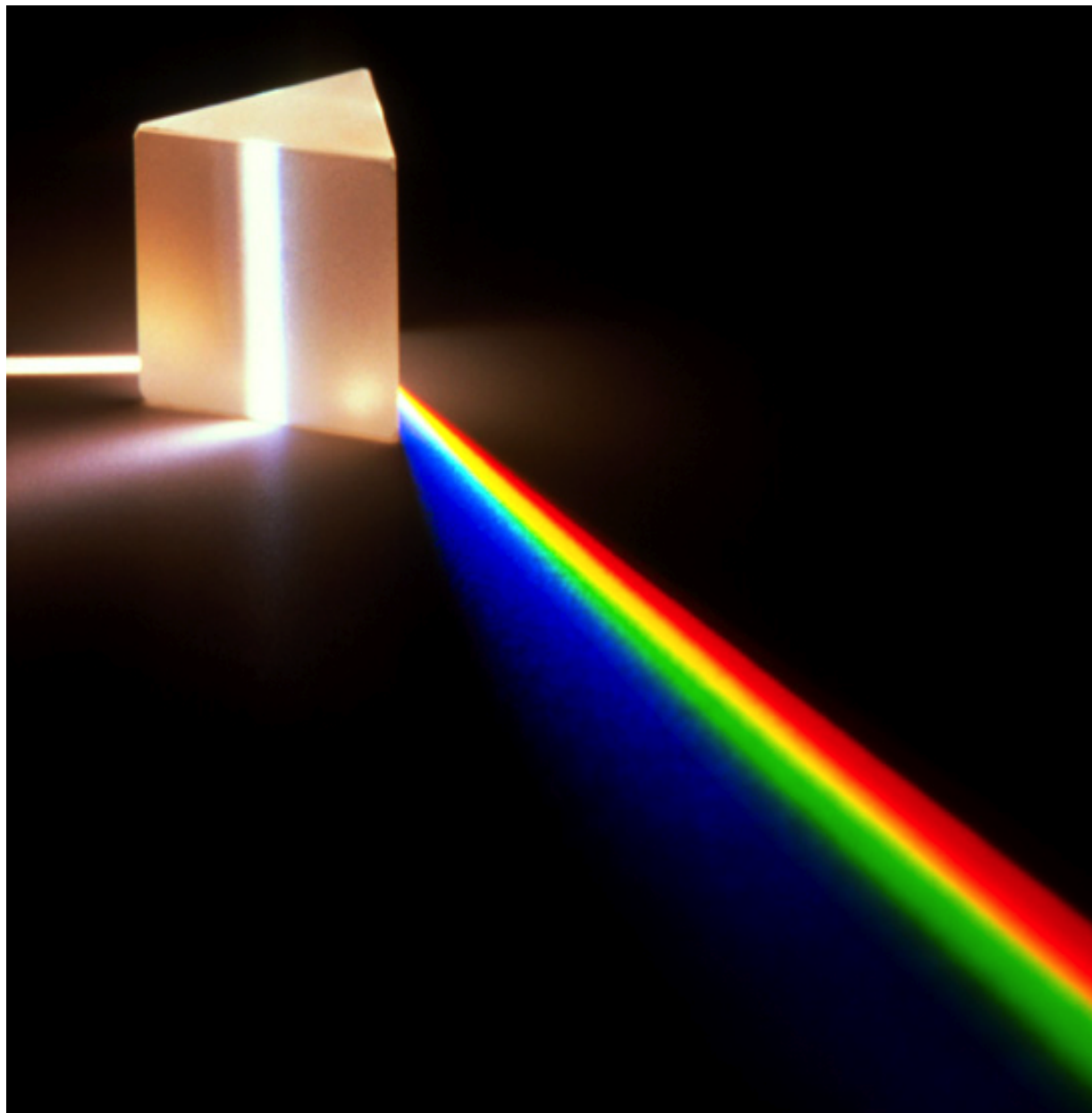
Quantum Measurement of a Single System

Orly Alter

Yoshihisa Yamamoto



Global Mathematical Vocabulary for Molecular Biological Discovery



Develop generalizations of the matrix and tensor decompositions that underlie the theoretical description of the physical world;

Create models that compare and integrate different types of large-scale molecular biological data;

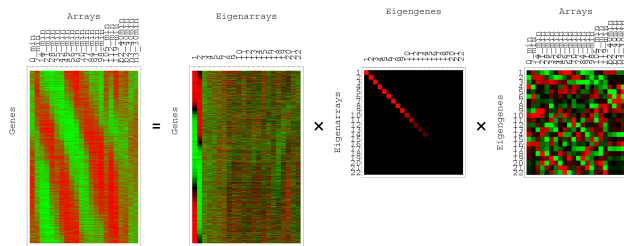
Predict global mechanisms that govern the activity of DNA and RNA.

Physics-Inspired Matrix (and Tensor) Models

Mathematical frameworks for the description of the data, in which the mathematical variables and operations might represent **biological reality**.

SVD

Alter, Brown & Botstein,
PNAS 97, 10101 (2000).

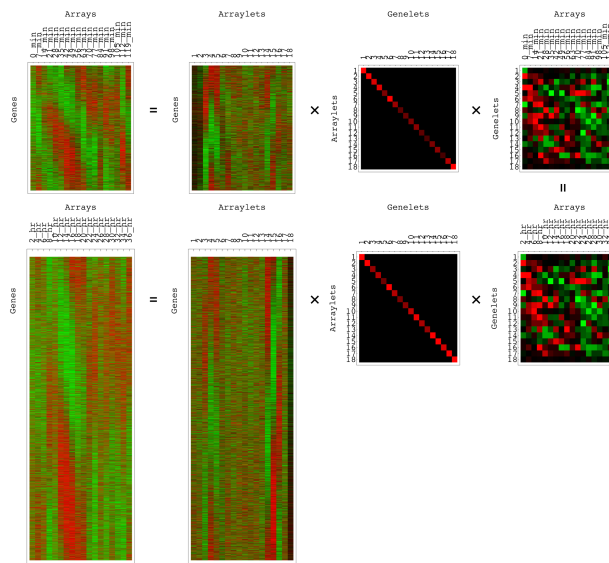


“Eigengenes” and
“eigenarrays” → cellular
processes and states
in a single dataset.

Eigenvalue Decomposition

Comparative GSVD

Alter, Brown & Botstein,
PNAS 100, 3351 (2003).

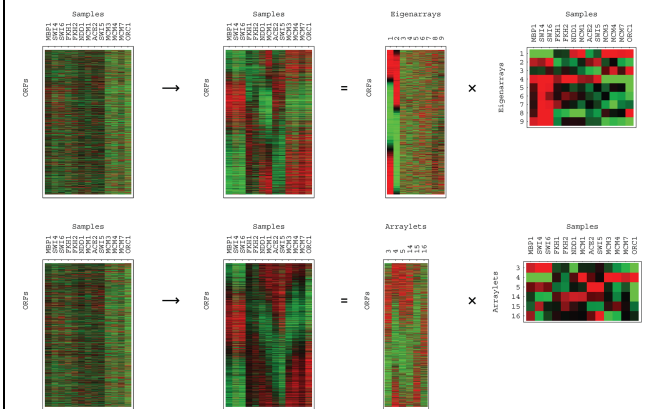


“Genelets” and
“arraylets” → phenomena
exclusive to one of, or
common to two datasets.

Generalized Eigenvalue
Decomposition

Integrative Pseudoinverse

Alter & Golub,
PNAS 101, 16577 (2004).

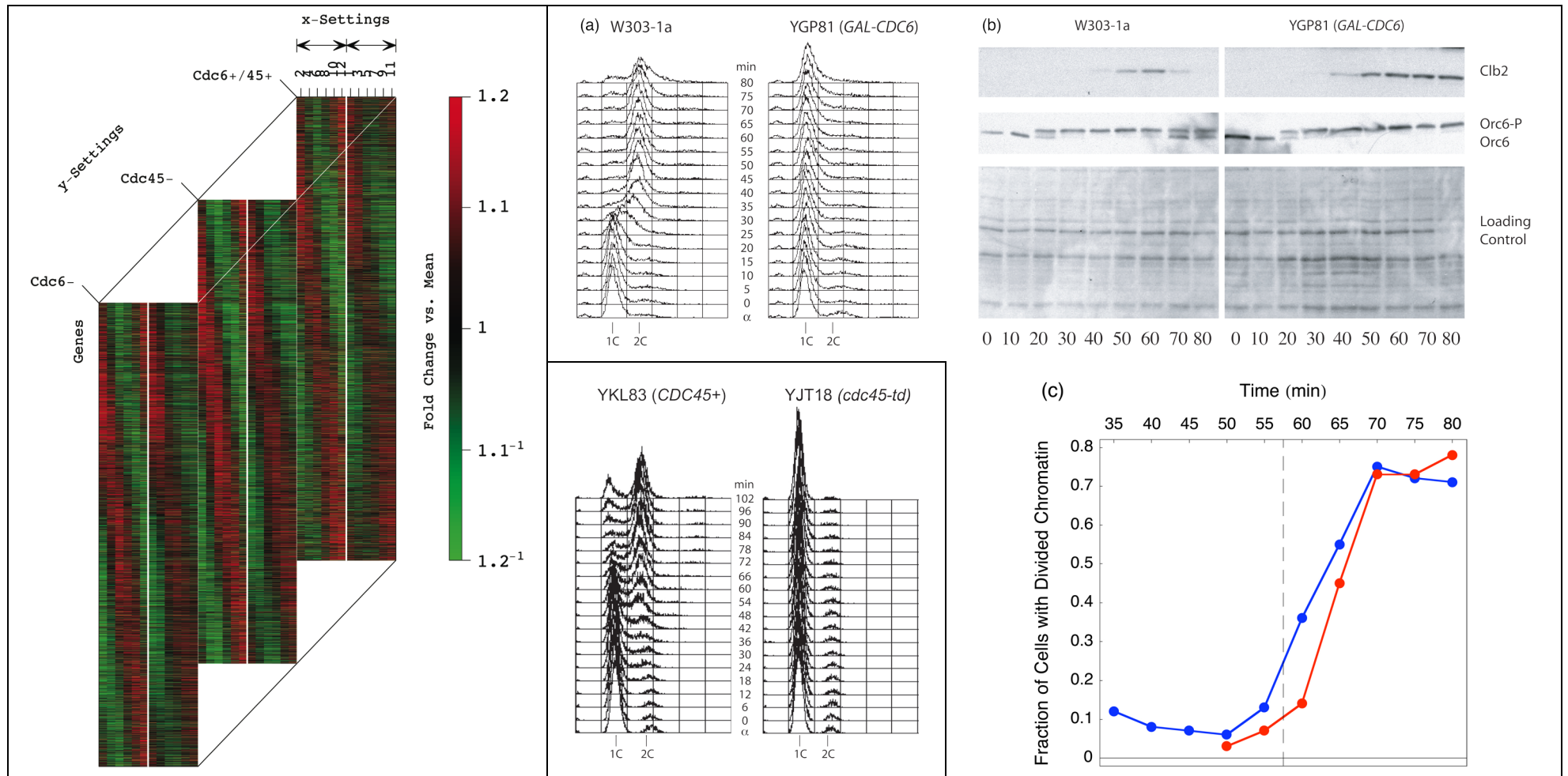


“Pseudoinverse
correlation” →
causal coordination
between two datasets.

Inverse Projection

Effects of DNA Replication on RNA Expression: Experimental Verification of a Computationally Predicted Mode of Regulation

Omberg, Meyerson, Kobayashi, Drury, Diffley & Alter, *MSB* 5, 312 (2009);
http://alterlab.org/verification_of_prediction/



Matrix and tensor modeling of large-scale molecular biological data can be used to correctly predict previously unknown cellular mechanisms.

HOSVD for Integrative Analysis of a High-Dimensional Dataset

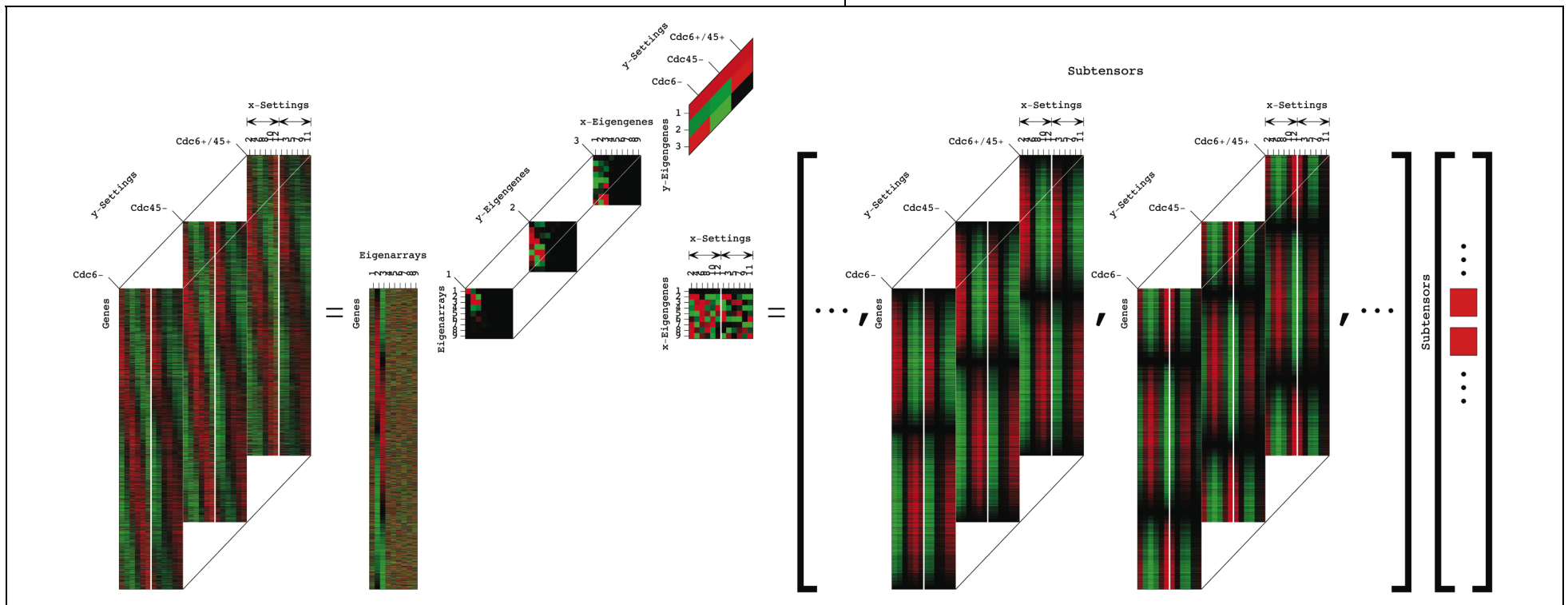
Omberg, Golub & Alter, *PNAS* 104, 18371 (2007); <http://alterlab.org/HOSVD/>

The data tensor is a **superposition** of all rank-1 “subtensors,” i.e., outer products of an eigenarray, an x - and a y -eigengene,

$$\mathcal{T} \equiv \sum_{a=1}^{LM} \sum_{b=1}^L \sum_{c=1}^M \mathcal{R}_{abc} \mathcal{S}(a, b, c).$$

The significance of a subtensor is defined by the corresponding “**fraction**,” computed from the higher-order singular values,

$$\mathcal{P}_{abc} \equiv \mathcal{R}_{abc}^2 / \sum_{a=1}^{LM} \sum_{b=1}^L \sum_{c=1}^M \mathcal{R}_{abc}^2.$$



De Lathauwer, De Moor & Vandewalle, *SIMAX* 21, 1253 (2000).

HOSVD for Integrative Analysis of a High-Dimensional Dataset

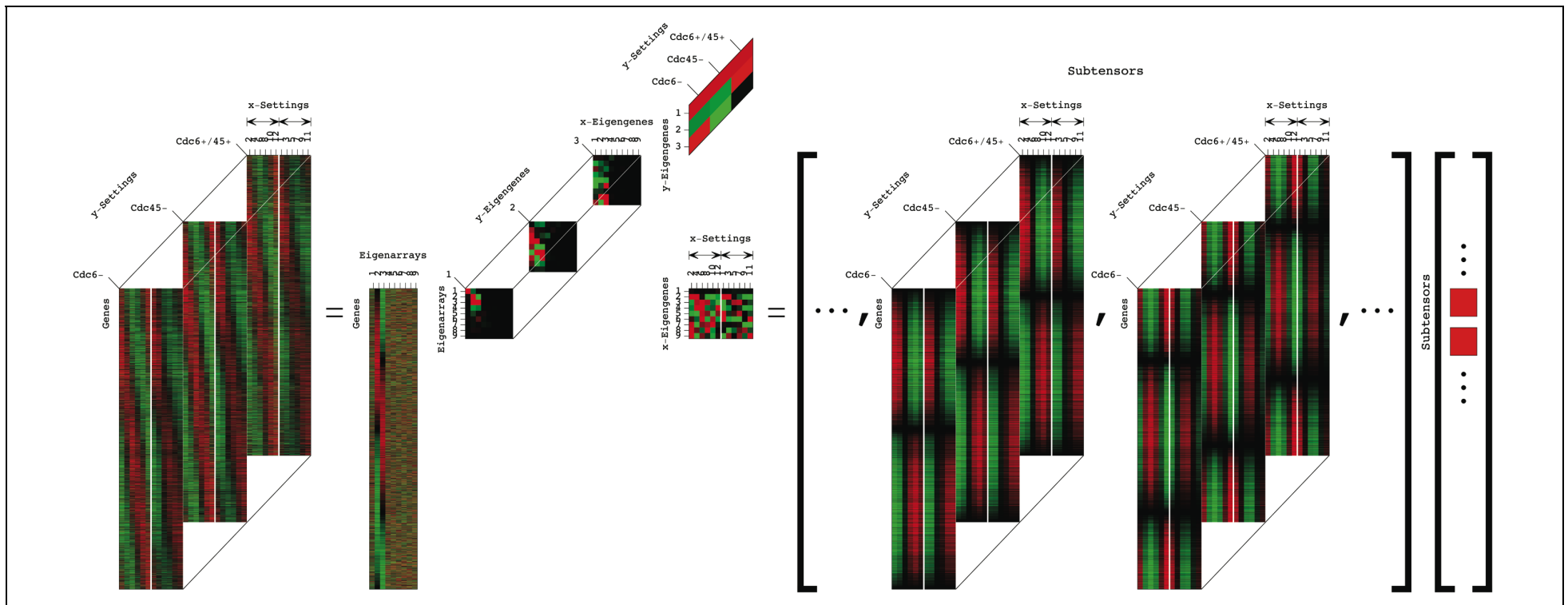
Omberg, Golub & Alter, *PNAS* 104, 18371 (2007); <http://alterlab.org/HOSVD/>

The complexity of the data is defined by the “normalized entropy,”

$$0 \leq d = \frac{-1}{2 \log(LM)} \sum_{a=1}^{LM} \sum_{b=1}^L \sum_{c=1}^M \mathcal{P}_{abc} \log(\mathcal{P}_{abc}) \leq 1.$$

A “degenerate subtensor space rotation” gives one unique subtensor,

$$\mathcal{R}_{a+k,b,c} \mathcal{S}(a+k,b,c) = \mathcal{R}_{abc} \mathcal{S}(a,b,c) + \mathcal{R}_{kbc} \mathcal{S}(k,b,c).$$

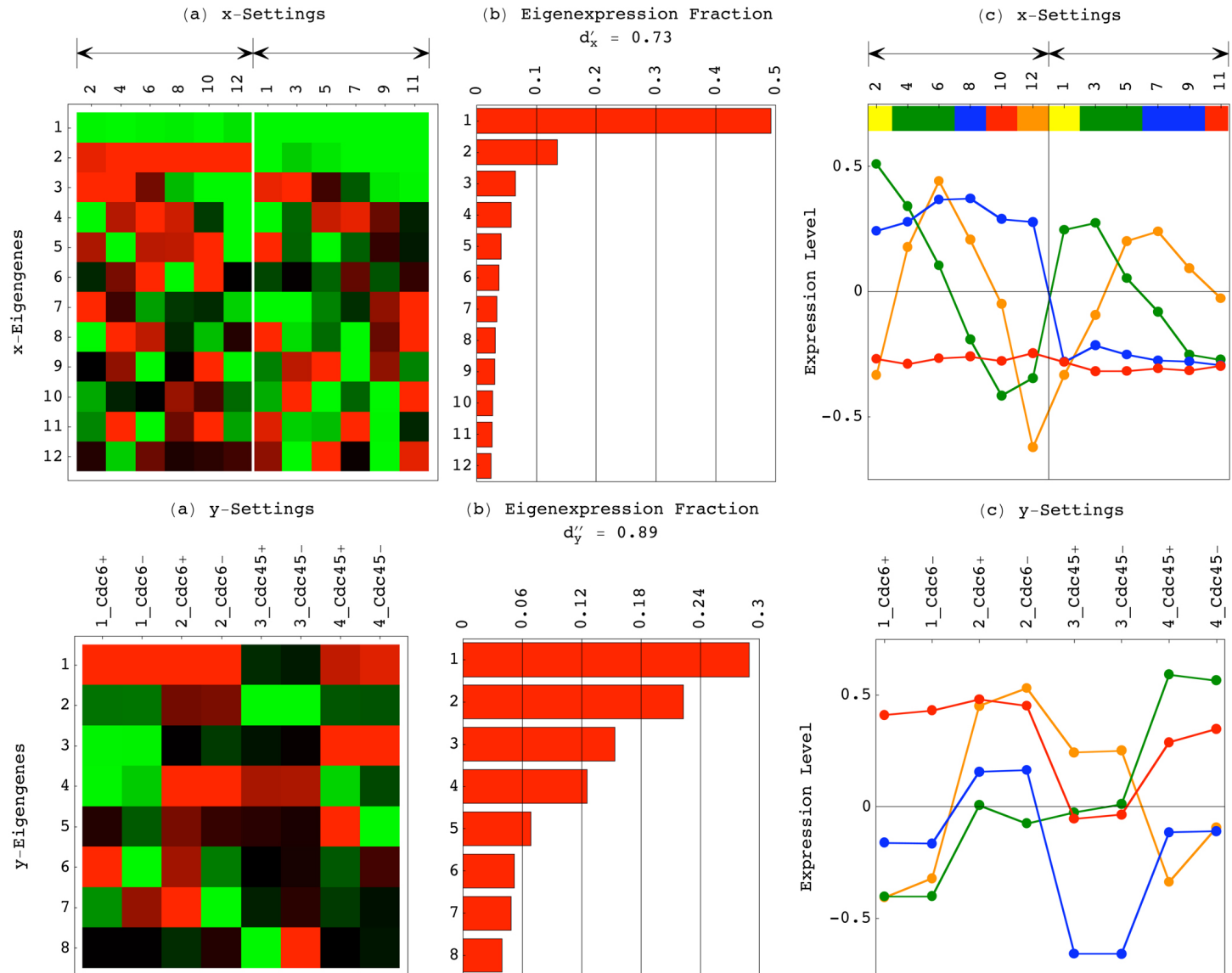


De Lathauwer, De Moor & Vandewalle, *SIMAX* 21, 1253 (2000).

HOSVD Detection and Removal of Artifacts

Reconstructing the data tensor of 4,270 genes \times 12 time points, or x -settings \times 8 time courses, or y -settings, filtering out “ x -eigengenes” and “ y -eigengenes” that represent experimental artifacts.

Batch-of-hybridization



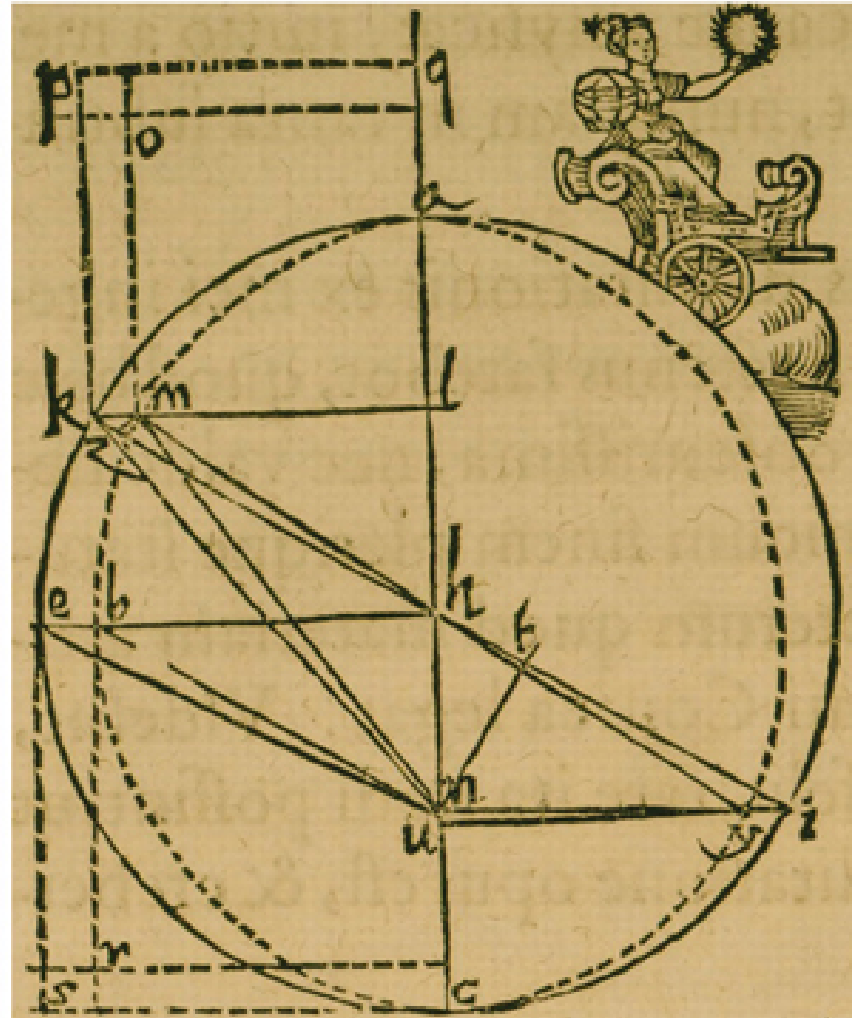
Culture batch, microarray platform and protocols

Patterns Underlie Principles of Nature: Global Correlations to Causal Coordination

Alter, *PNAS* 103, 16063 (2006);

Alter, in *Microarray Data Analysis: Methods and Applications* (Humana Press, 2007), pp. 17–59.

	Tempus	Locus ☉	10 ⁴ x Temp distantia	Magni a Sole distantia
P A R S Q U A R T A.	1582. 23 Nove.H.16. 0	11.41 ♀	98345	158852
	26 Dece.H. 8.30	15. 4 ♀	98226	162104
	30 Dece.H. 8.10	19. 9 ♀	98252	162443
	1583. 26 Janua.H. 6.15	16.33 =	98624	164421
	1584. 21 Dece.H.14. 0	10.16 ♀	98207	164907
	1585. 24 Janua.H. 9. 0	14.53 =	98595	166210
	4 Febr.H. 6.40	26.10 =	98830	166400
	12 Mart.H.10.30	2.16 ♀	99858	166170
	1587. 25 Janua.H.17. 0	16. 1 =	98611	166232
	4 Mart.H.13.24	24 0 X	99595	164737
	10 Mart.H.11.30	29.52 X	99780	164382
	21 April.H. 9.30	10.48 ♀	101010	161027
1589. 8 Mart.H.16.24	28.36 X	99736	161000	
13 April.H.11.15	3.38 ♀	100810	157141	
15 April.H.12. 5	5.36 ♀	100866	156900	
6 Maji.H.11.20	25.49 ♀	101366	154326	
1591. 13 Maji.H.14. 0	2.10 II	101467	147891	
6 Junii H.12.20	24.59 II	101769	144981	
10 Junii H.11.50	28.47 II	101789	144526	
28 Junii H.10.24	15.51 =	101770	142608	
1593. 21 Julii H.14. 0	8.26 II	101498	138376	
22 Aug.H.12.20	9.11 ♀	100761	138463	
29 Aug.H.10.20	11.54 ♀	100562	138682	
3 Octo.H. 8. 0	20.15 ♀	99500	140697	
1595. 17 Sept.H.16.45	4.18 ♀	99990	143212	
27 Octo.H.12.20	13.59 =	98851	147890	
3 Nove.H.12. 0	21. 2 =	98694	148773	
18 Dece.H. 8. 0	6.43 ♀	98200	154519	

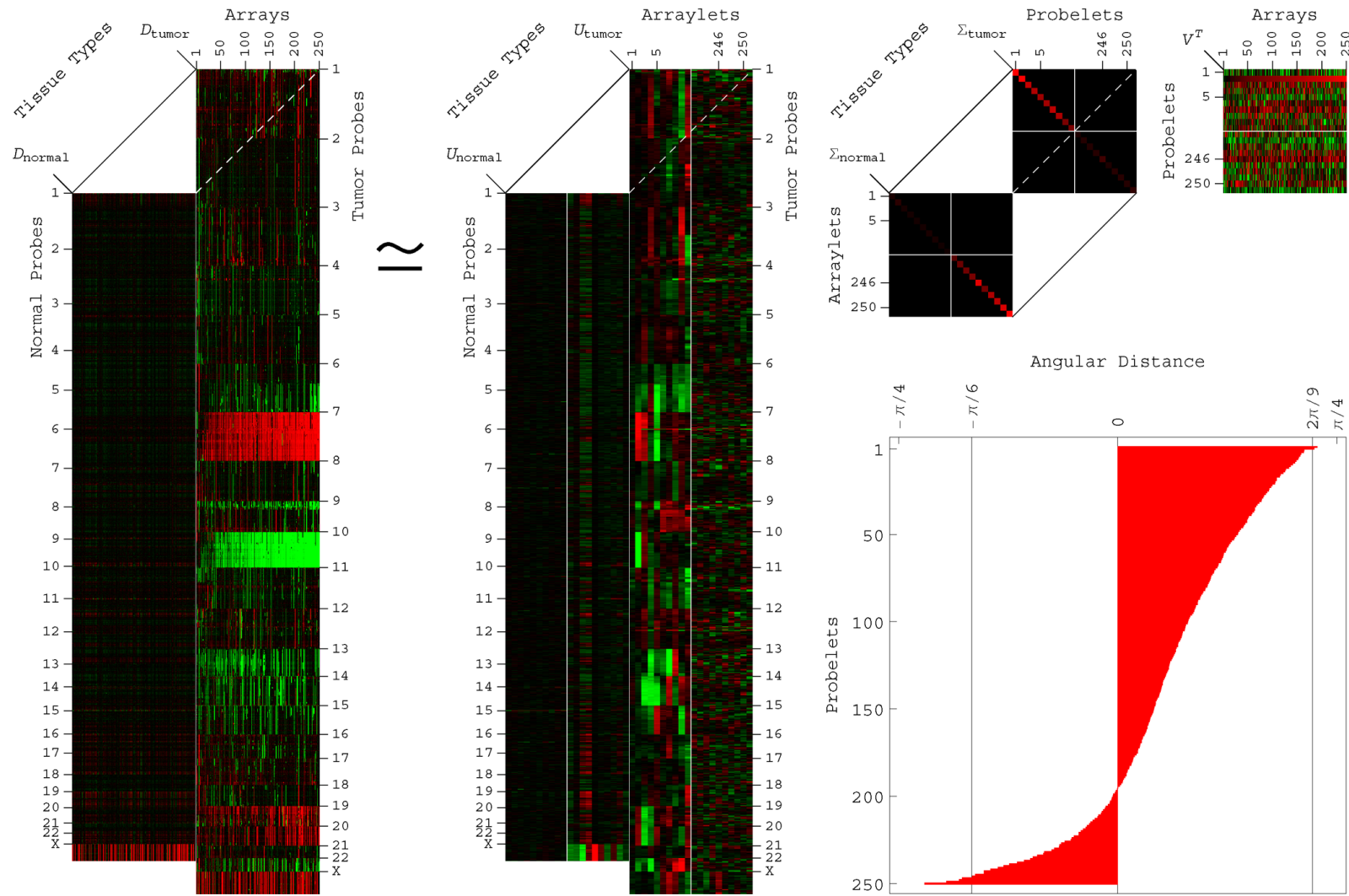


Kepler's discovery of his first law of planetary motion from mathematical modeling of Brahe's astronomical data.

Kepler, *Astronomia Nova* (Voegelinus, Heidelberg, 1609).

Computational Discovery and Validation of a Genomic Predictor of GBM Survival

Lee,* Alpert,* Sankaranarayanan & Alter, *PLoS One* 7, e30098 (2012);
http://alterlab.org/GBM_prognosis/



The number of large-scale datasets recording multiple aspects of a single phenomenon is increasing in many areas, e.g., personalized medicine.

GSVD for Comparative Analysis of Two Different Two-Dimensional Datasets

Alter, Brown & Botstein, *PNAS* 100, 3351 (2003); <http://alterlab.org/GSVD/>

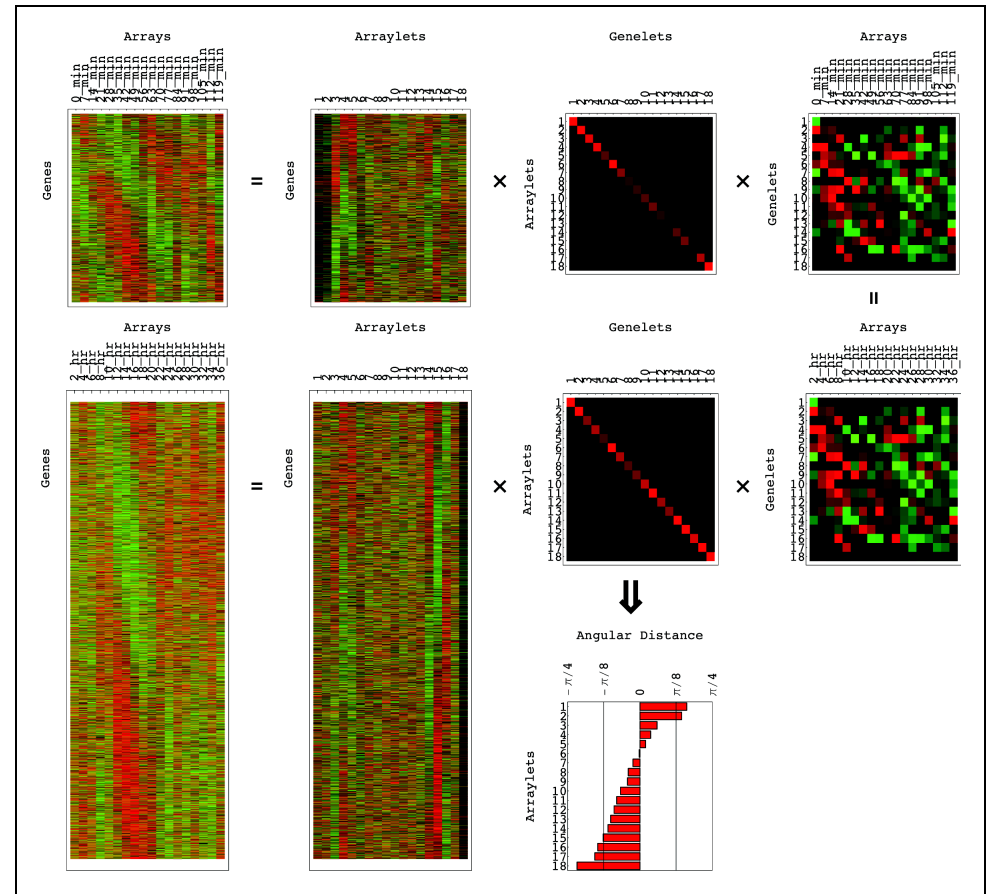
The GSVD **simultaneously separates the two datasets** into paired weighted sums of outer products, of each normalized right basis vector, or a “probelet” (a pattern of variation across the patients), which is identical for both datasets, **combined with one of the two corresponding orthonormal left basis vectors, or “arraylets”** (the tumor- and normal-specific patterns of variation across the genome),

$$D_i = U_i \Sigma_i V^T = \sum_{n=1}^N \sigma_{i,n} u_{i,n} \otimes v_n^T, \quad i = 1, 2.$$

The significance of a probelet and its corresponding arraylet in one dataset relative to the second is defined by the “**angular distance,**”

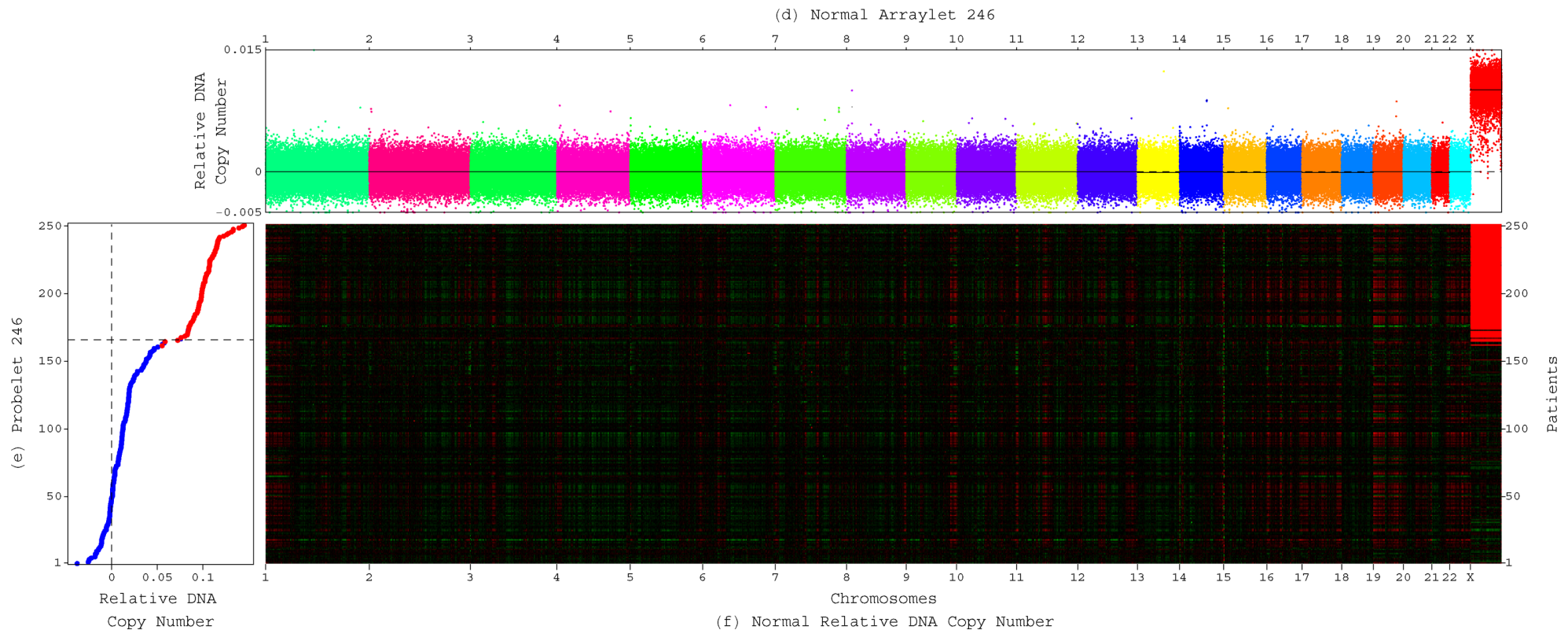
$$-\pi/4 \leq \arctan(\sigma_{1,n} / \sigma_{2,n}) - \pi/4 \leq \pi/4.$$

Van Loan, *SINUM* 13, 76 (1976); Paige & Saunders, *SINUM* 18, 398 (1981);
Van Loan, *Numer Math* 46, 479 (1985).



Copy-Number Variations (CNVs) Common to the GBM Tumor and Normal Brain

GSVD identifies CNVs that occur in the normal human genome and are preserved in the GBM tumors, e.g., female-specific X chromosome amplification, without a-priori knowledge of these variations.



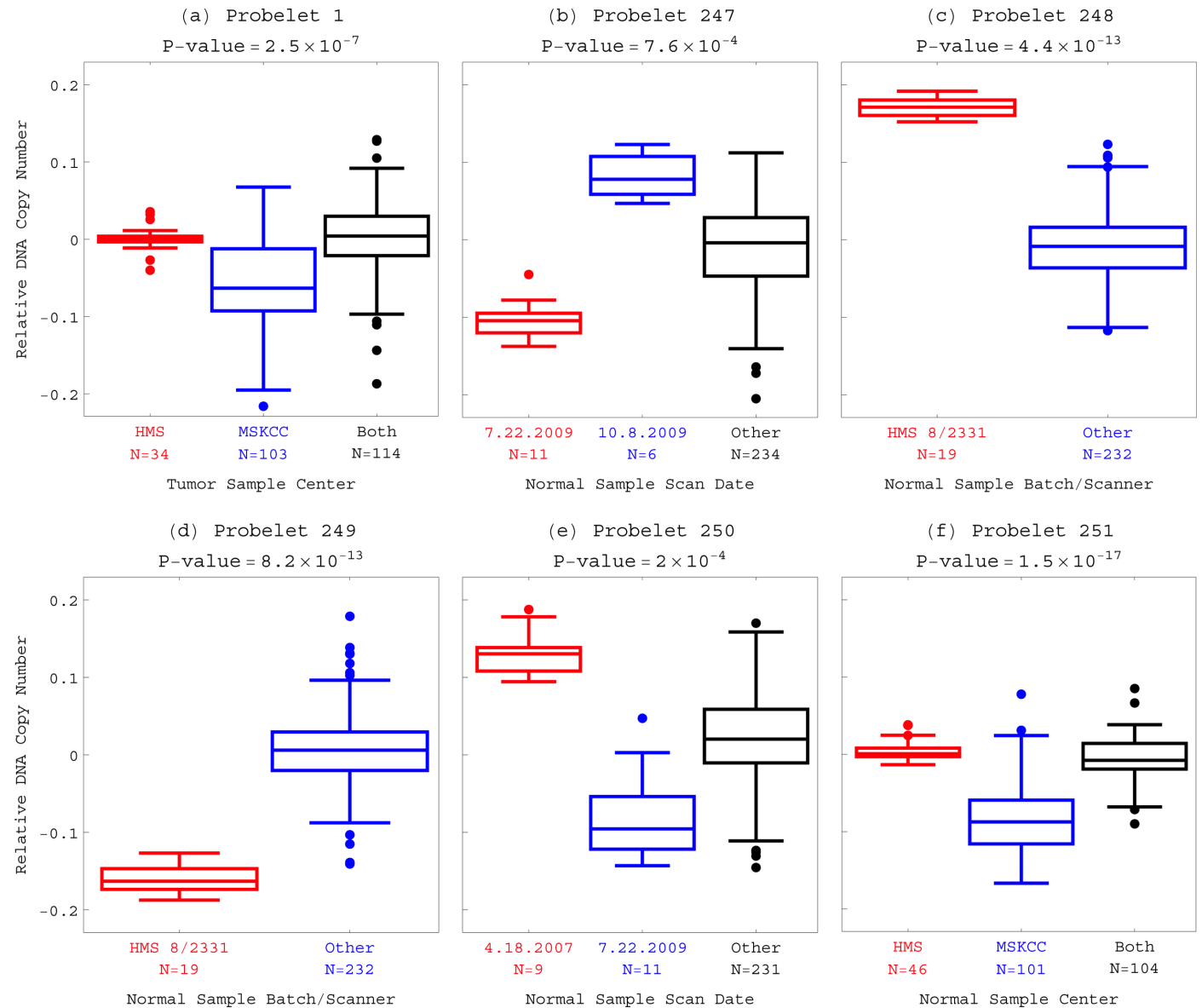
Patients' gender is correctly identified also where the TCGA database entries and the copy-number gender assignments are in discrepancy.

NHGRI's Interest in Applications to Analyze and Develop Methods for X Chromosome Genome-wide Association (GWA) Data; <http://grants.nih.gov/grants/guide/notice-files/NOT-HG-11-021.html>

Experimental Variations

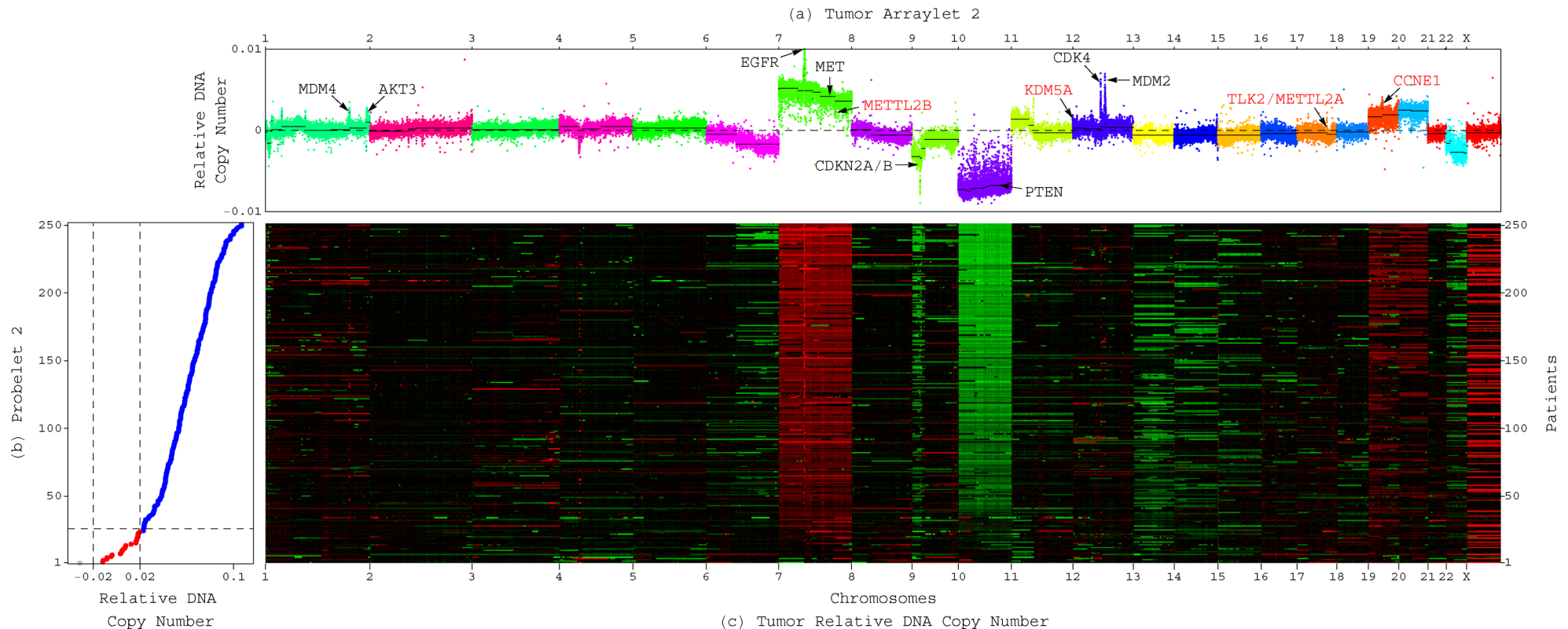
Exclusive to the Tumor or Normal Profiles

GSVD identifies experimental variations, e.g., in tissue batch, genomic center, hybridization date and scanner.



Global Pattern of Tumor-Exclusive Copy-Number Alterations Predicts Drug Targets

Lee & Alter, 60th Annual Meeting of the ASHG (Washington, DC, November 2–6, 2010).



The pattern includes most known GBM-associated changes in chromosome numbers and focal copy-number alterations (CNAs), as well as several previously unreported CNAs in >3% of the patients: the biochemically putative drug target, cell cycle-regulated serine/threonine kinase-encoding *TLK2*, the tRNA methyltransferase *METTL2A*, and the cyclin E1-encoding *CCNE1*.

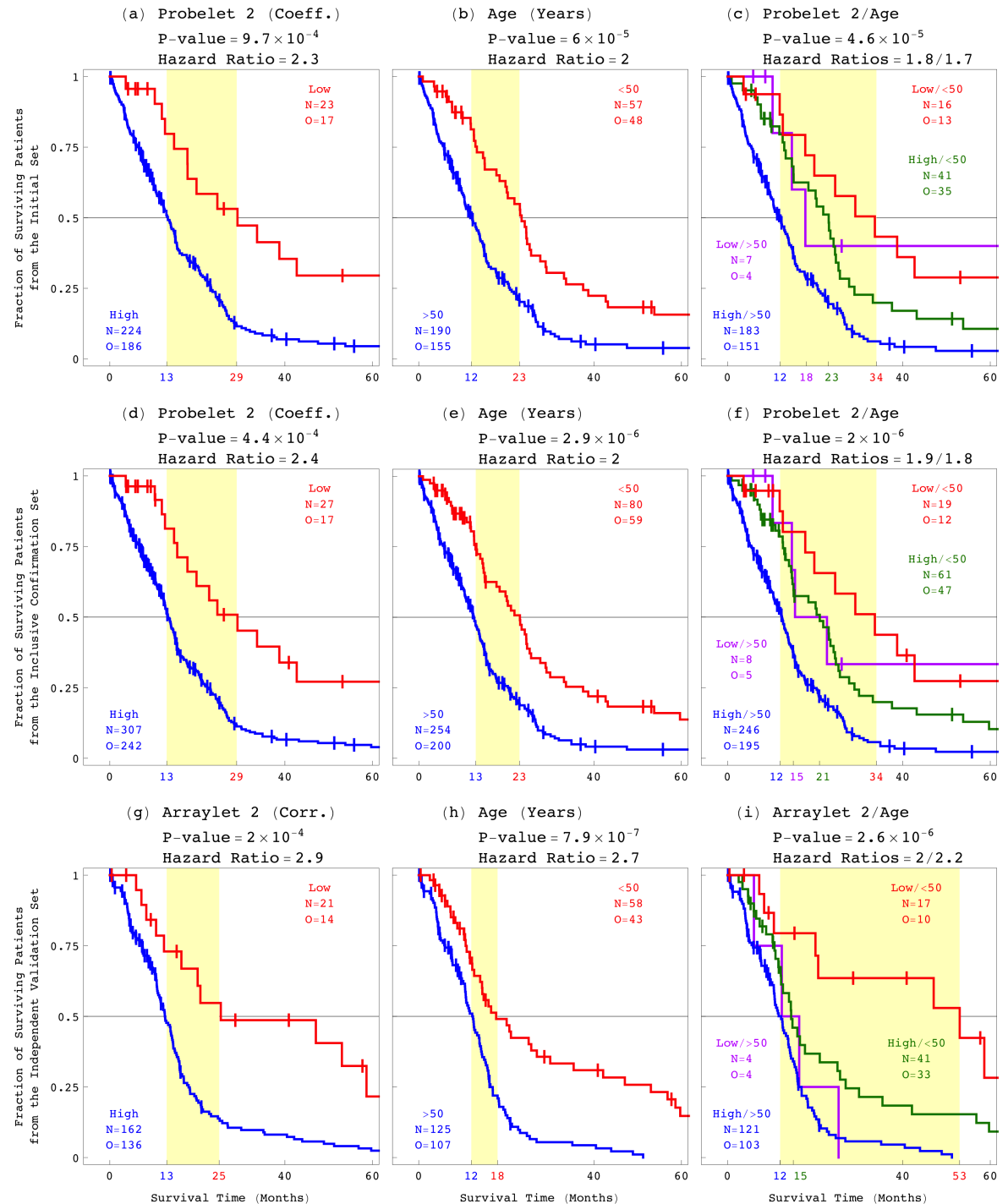
Global, Genomic Predictor of GBM Survival

The global pattern is correlated with, and possibly causally related to, brain cancer survival.

The GBM survival phenotype is the outcome of its global genotype.

Despite recent large-scale profiling efforts, the best prognostic indicator of GBM prior to the discovery of this pattern was the patient's age at diagnosis.

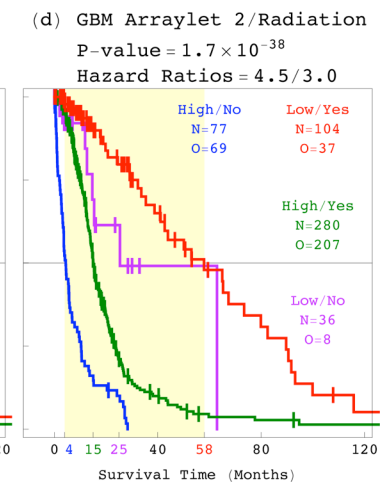
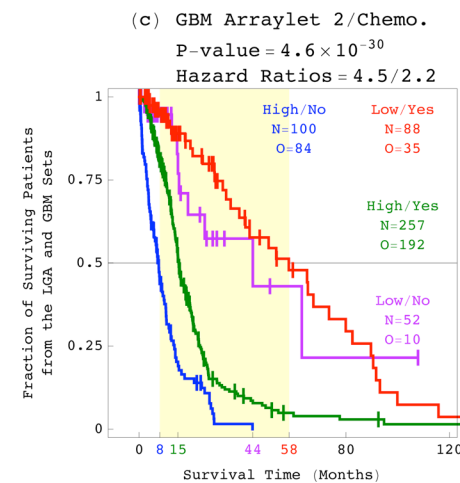
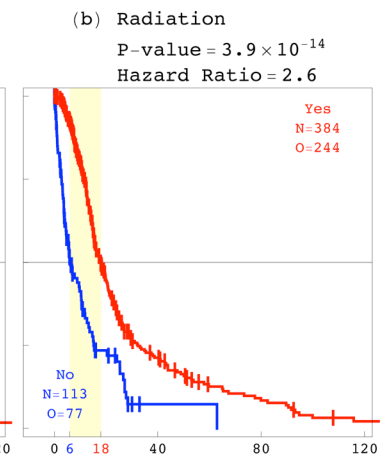
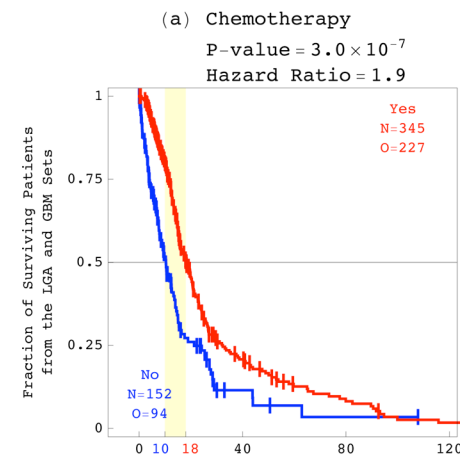
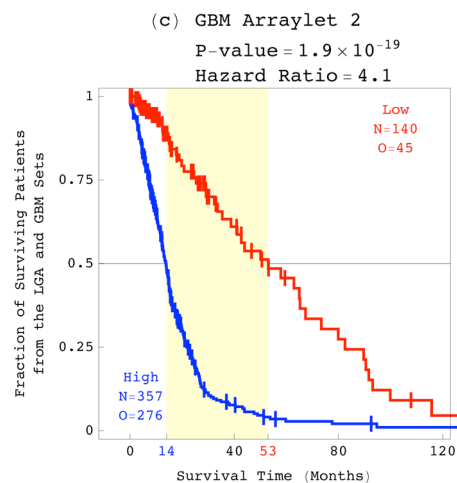
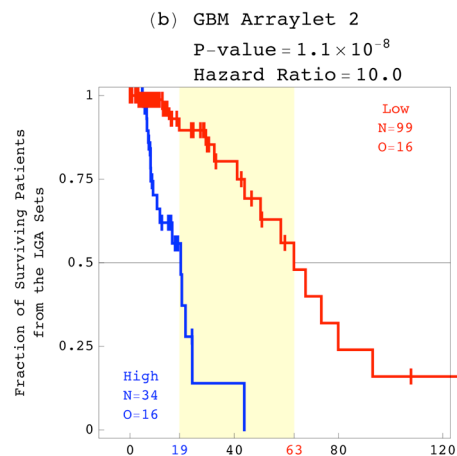
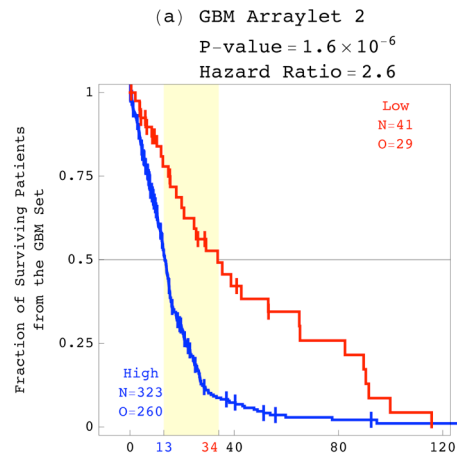
The pattern performs as well as age, and is independent of age, such that combined with age it makes a better predictor than age alone.



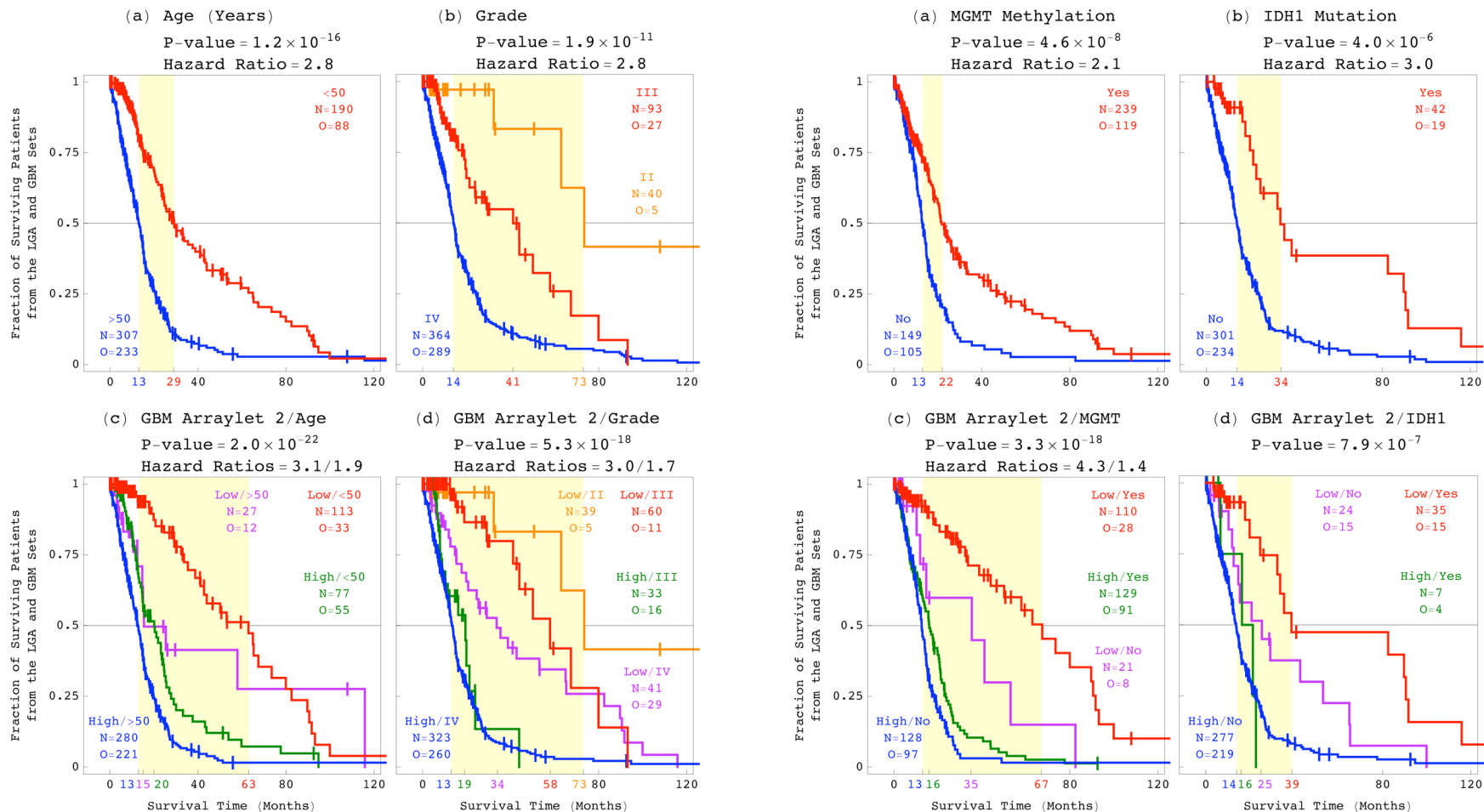
Platform-Independent Genomic Predictor of Astrocytoma Outcome

Aiello & Alter, under review;
 Aiello & Alter, *BMES Annual Meeting* (Tampa, FL, October 7–10, 2015).

The GBM pattern identifies among grades III and II, i.e., lower-grade astrocytoma (LGA) patients a subtype, statistically indistinguishable from that among the GBM patients, where the CNA genotype is correlated with a one-year survival phenotype.



Statistically Better Than, and Independent of Age, Grade, and Laboratory Tests



Recurring DNA CNAs were observed in astrocytoma tumors' genomes for decades, however, copy-number subtypes predictive of patients' outcomes were not identified before, despite the growing number of datasets recording different aspects of the disease, and due to a need for frameworks that can simultaneously find similarities and dissimilarities across the datasets.

Computational Discovery and Validation of Genomic Predictors of OV Outcome

Sankaranarayanan,* Schomay,* Aiello & Alter,
PLoS One 10, e121396 (2015);
http://alterlab.org/OV_prognosis/

$$\mathcal{D}_i = \mathcal{R}_i \times_a U_i \times_b V_x \times_c V_y$$

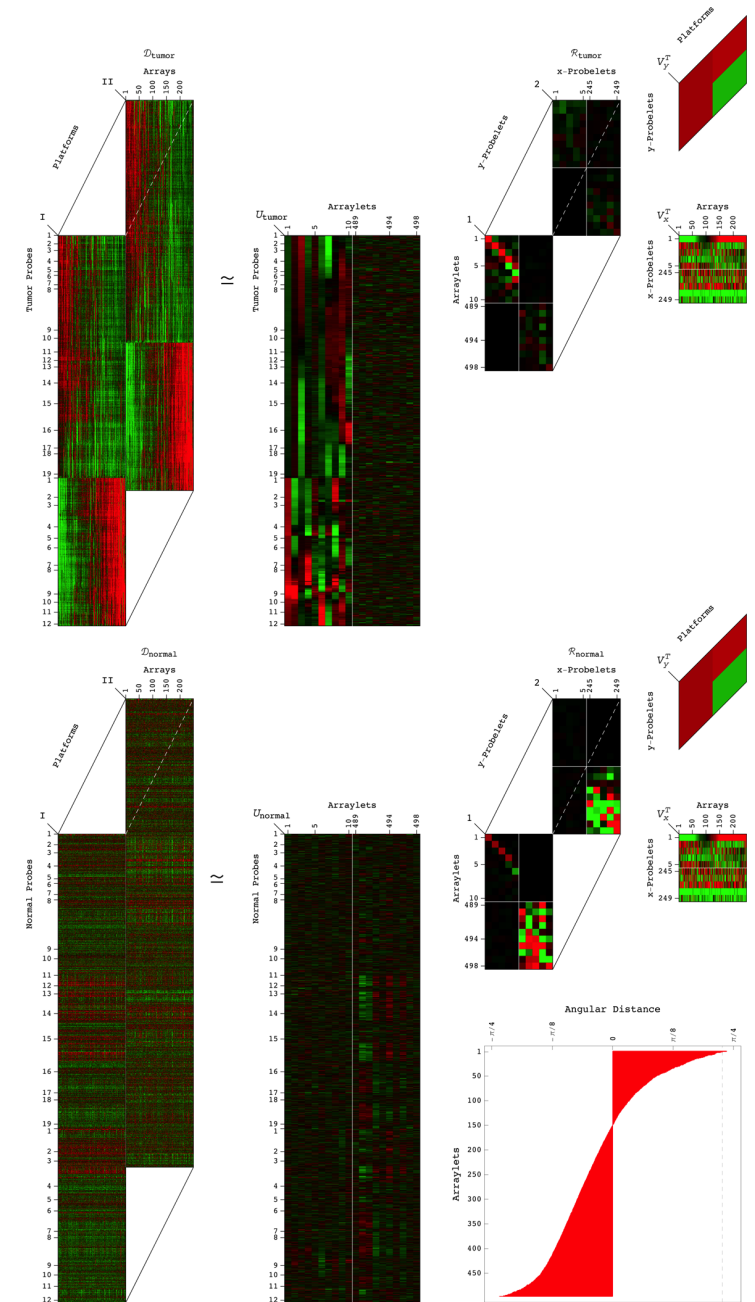
$$= \sum_{a=1}^{LM} \sum_{b=1}^L \sum_{c=1}^M \mathcal{R}_{i,abc} \mathcal{S}_i(a,b,c),$$

$$\mathcal{S}_i(a,b,c) = u_{i,a} \otimes v_{x,b}^T \otimes v_{y,c}^T$$

$i = 1, 2.$

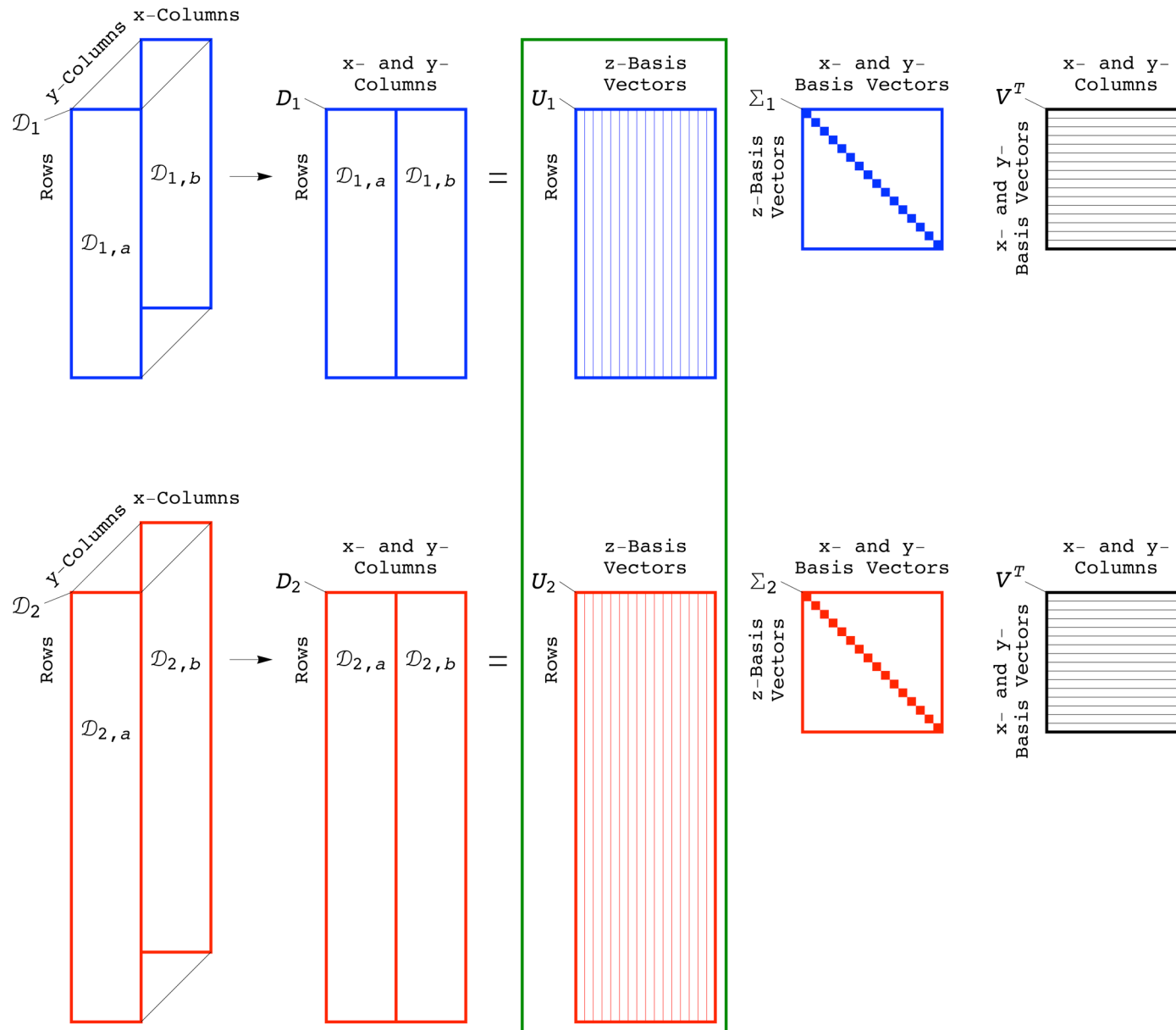
This exact decomposition extends the GSVD and the tensor HOSVD from a decomposition of either two column-matched matrices or one tensor, respectively, to a decomposition of two order-matched, column-matched, and row-independent tensors.

Omberg, Golub & Alter, *PNAS* 104, 18371 (2007);
<http://alterlab.org/HOSVD/>



Tensor GSVD for Comparative Analysis of Two Different High-Dimensional Datasets

Schomay, Aiello & Alter, in preparation; Schomay, Aiello & Alter, 2016 *Tensor Decompositions and Applications Workshop* (Leuven, Belgium, January 18–22, 2016).



Tensor GSVD for Comparative Analysis of Two Different High-Dimensional Datasets

Schomay, Aiello & Alter, in preparation;
Schomay, Aiello & Alter, *SIAM Annual Meeting* (Chicago, IL, July 7–11, 2014).

The mathematical properties of the tensor GSVD allow interpreting its variables and operations in terms of the similar as well as dissimilar, e.g., biomedical reality between the datasets.

Supplementary Lemma 1:

The tensor GSVD exists for two tensors of the same order since it is constructed from the GSVDs of the tensors unfolded into full column rank matrices.

Supplementary Lemma 2:

The tensor GSVD has the same uniqueness properties as the GSVD.

Supplementary Corollary 1:

The tensor GSVD of two second-order tensors reduces to the GSVD of the corresponding matrices.

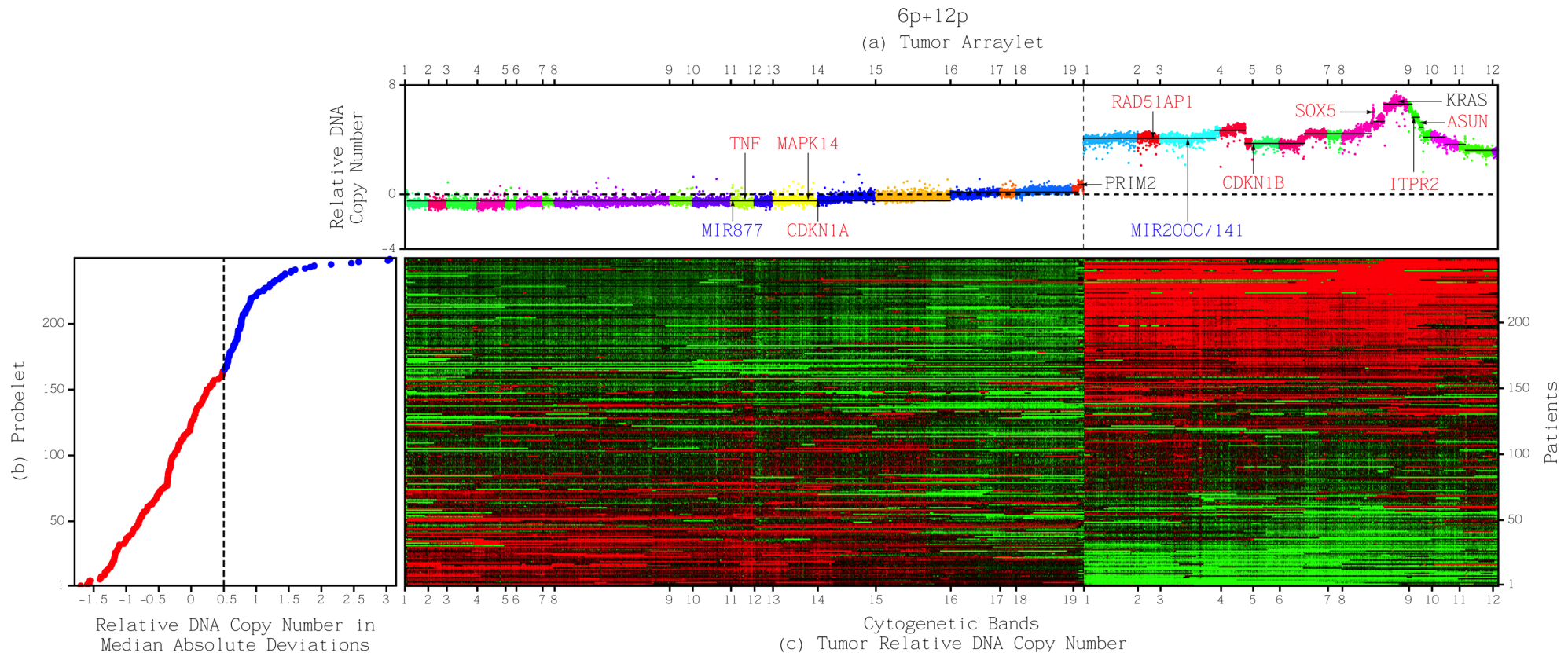
Supplementary Theorem 1:

The tensor GSVD of the tensor, which row mode unfolding gives the identify matrix, and a tensor of the same column dimensions reduces to the HOSVD of the tensor.

Theorem 1:

The tensor GSVD angular distance equals that of the row mode GSVD.

Chromosome Arm-Wide Patterns of Tumor-Exclusive Platform-Consistent Alterations Encoding for Cell Transformation



Loss of the p21-encoding *CDKN1A* and the p38-encoding *MAPK14* on 6p, and gain of *KRAS* on 12p, combined but not separately, can lead to transformation of human normal to tumor cells. There exist drugs that interact with *CDKN1A*, *MAPK14*, and *RAD51AP1*.

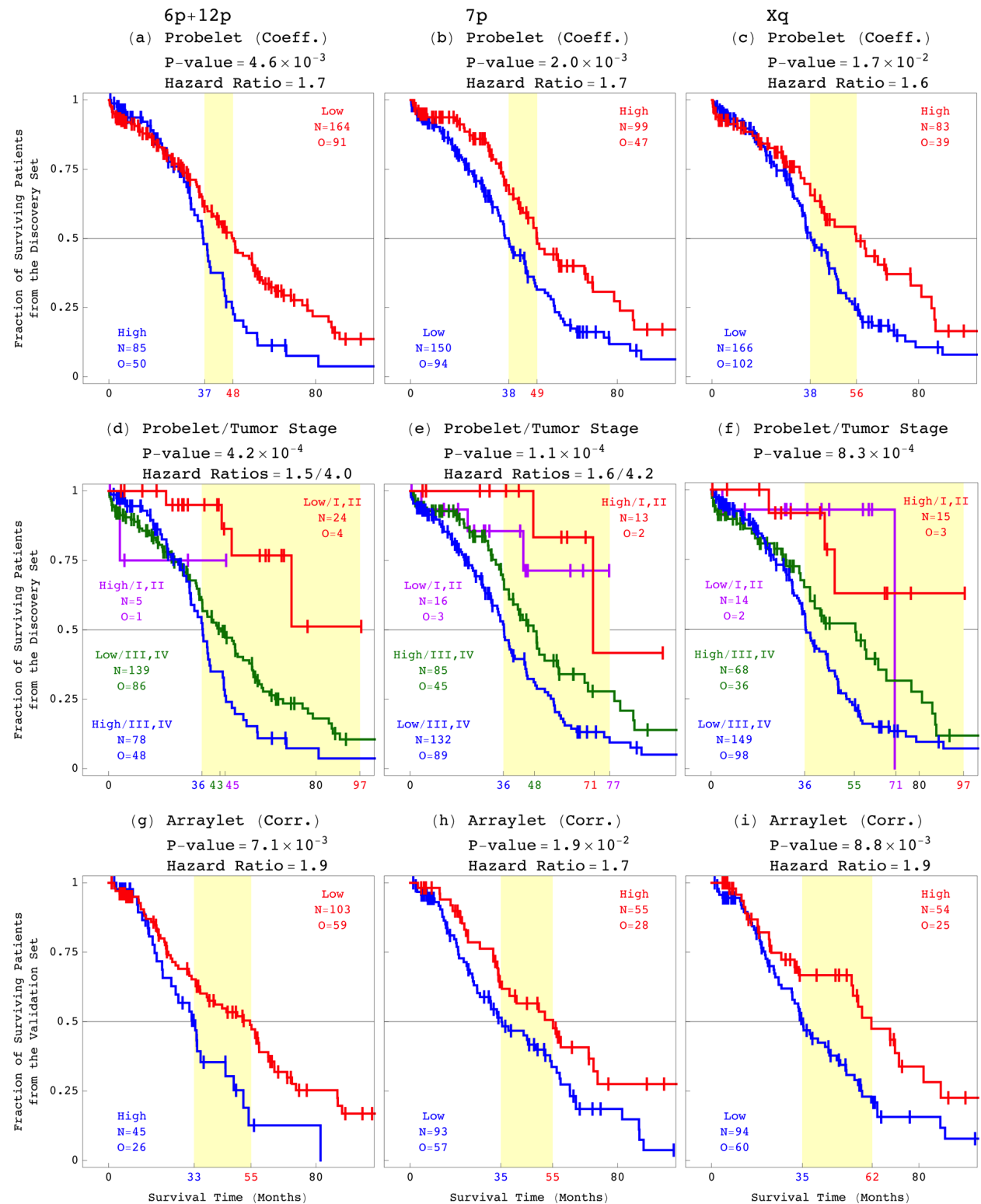
Hahn, Counter, Lundberg, Beijersbergen, Brooks & Weinberg, *Nature* 400, 464 (1999).

Predictors of OV Survival

Chromosome arm-wide patterns are correlated with, and possibly causally related to, ovarian cancer survival.

Despite recent large-scale profiling efforts, the best prognostic indicator of OV prior to the discovery of these patterns was the tumor's age at diagnosis.

The patterns are independent of stage, and combined with stage make better predictors than stage alone.



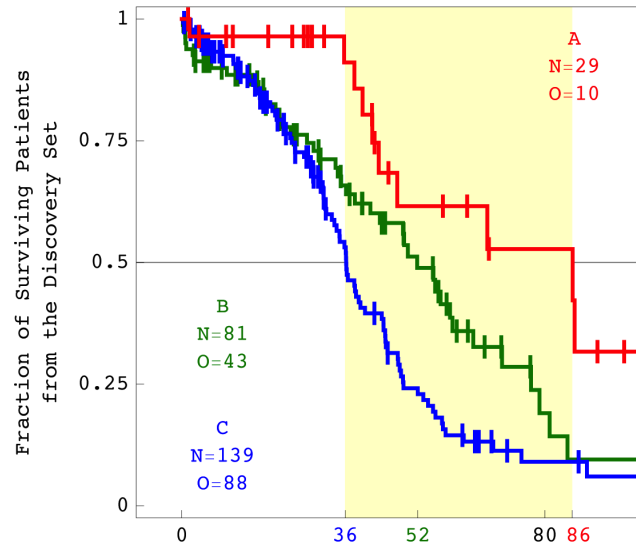
Predictors of OV Survival and Response to Platinum-Based Chemotherapy

~25% of primary OV tumors are resistant, and most recurrent OV tumors develop resistance to platinum-based chemotherapy, the first-line treatment for >30 years.

There exist drugs for resistant tumors, but no pathology laboratory diagnostic exists that distinguishes between resistant and sensitive tumors before the treatment.

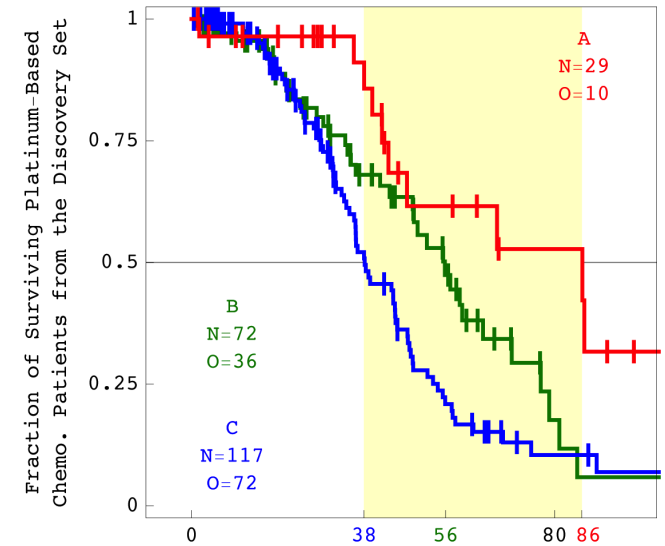
(a) Three Probelets (Comb.)

P-value = 1.4×10^{-4}



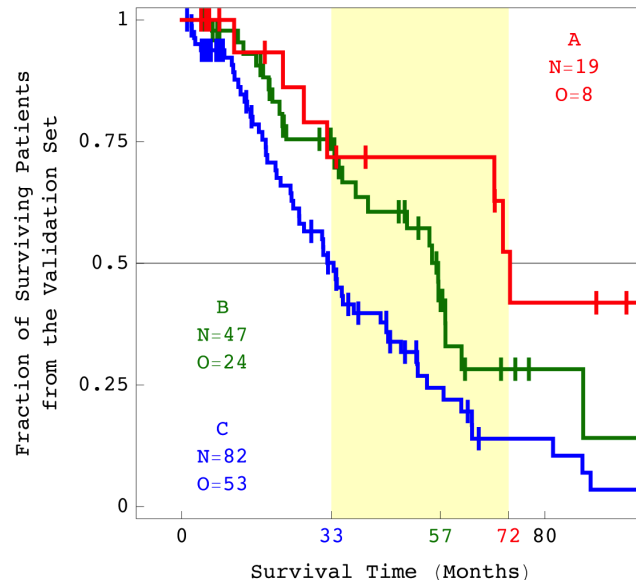
(b) Three Probelets (Comb.)

P-value = 6.5×10^{-4}



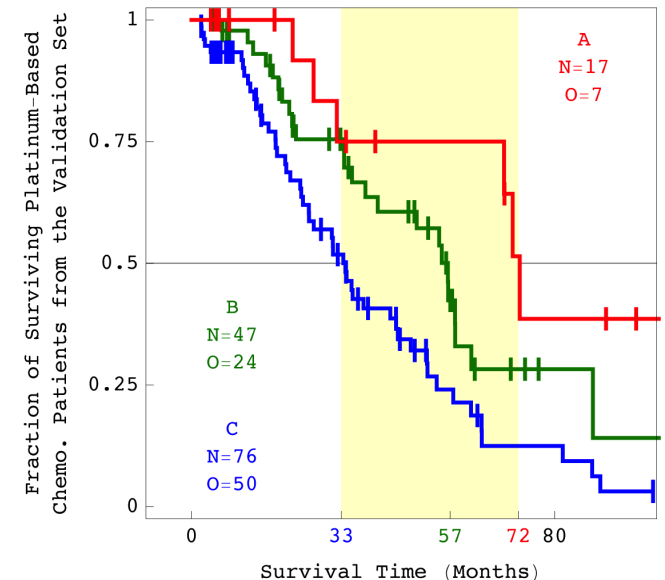
(c) Three Arraylets (Comb.)

P-value = 8.1×10^{-4}



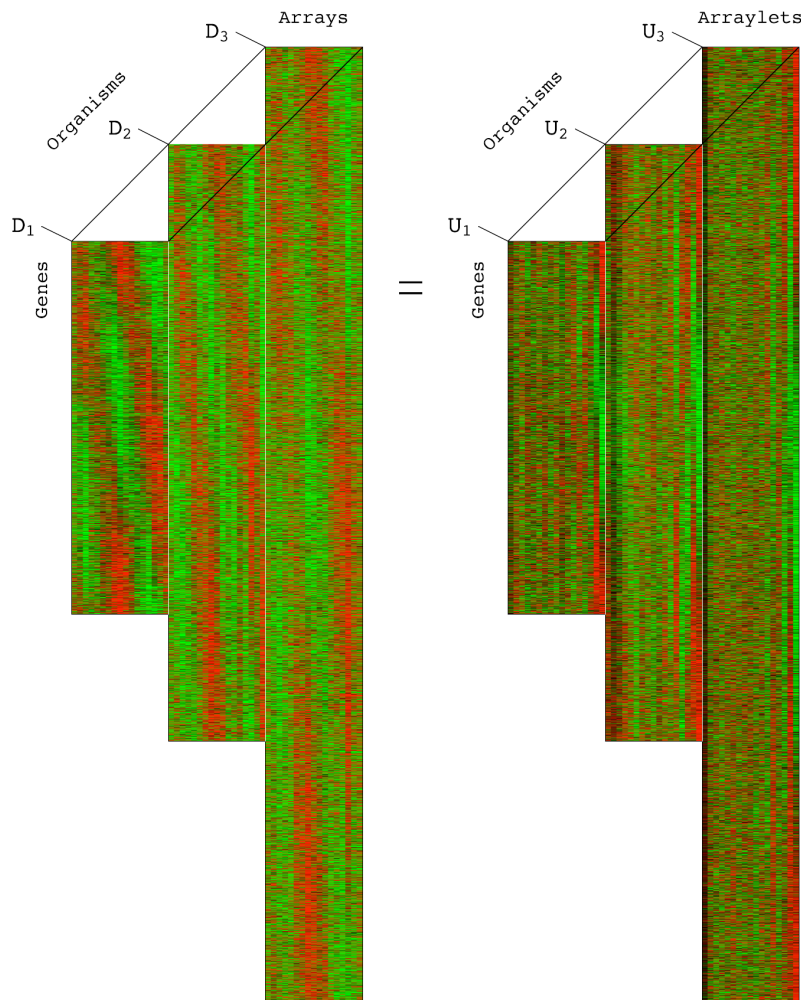
(d) Three Arraylets (Comb.)

P-value = 1.0×10^{-3}



HO GSVD for Comparative Analysis of Multiple Two-Dimensional Datasets

Ponnappalli, Golub & Alter, *Stanford University and Yahoo! Research Workshop on Algorithms for Modern Massive Datasets* (Stanford, CA, June 21–24, 2006).



Definition:

$$D_i = U_i \Sigma_i V^T, \quad \Sigma_i = \text{diag}(\sigma_{i,k})$$

$$SV = V\Lambda$$

$$S \equiv \frac{1}{N(N-1)} \sum_{i=1}^N \sum_{j>i}^N (A_i A_j^{-1} + A_j A_i^{-1})$$

$$= \frac{2}{N(N-1)} \sum_{i=1}^N \sum_{j>i}^N S_{ij}$$

$$A_i = D_i^T D_i, \quad S_{ij} = \frac{1}{2} (A_i A_j^{-1} + A_j A_i^{-1})$$

Assumption: $D_i \in \mathcal{R}^{m_i \times n}$

The matrix V , identical in all factorizations, is obtained from the balanced eigensystem of S , which does not depend upon the ordering of D_i .

HO GSVD for Comparative Analysis of Multiple Two-Dimensional Datasets

Ponnappalli, Saunders, Van Loan & Alter, *PLoS One* 6, e28072 (2011); http://alterlab.org/HO_GSVD/

This exact decomposition extends to higher orders all of the mathematical properties of the GSVD except for complete orthogonality of U_i for all i .

Supplementary Theorems 1–5:

For $N=2$, our HO GSVD leads algebraically to the GSVD.

Theorem 1: S has n independent eigenvectors, and the eigenvectors and eigenvalues of S are real.

Theorem 2: The eigenvalues of S satisfy $\lambda_k \geq 1$.

Theorem 3: **The common HO GSVD subspace.** An eigenvalue satisfies $\lambda_k=1$ if and only if the corresponding right basis vector v_k is of equal significance in all matrices D_i and D_j , i.e., $\sigma_{i,k} / \sigma_{j,k} = 1$ for all i and j , and the corresponding left basis vector $u_{i,k}$ is orthonormal to all other left basis vectors in U_i for all i .

Corollary 1: An eigenvalue satisfies $\lambda_k=1$ if and only if the corresponding right basis vector v_k is a generalized singular vector of all pairwise GSVD factorizations of the matrices D_i and D_j with equal corresponding generalized singular values for all for all i and j .

Supplementary Theorem 6 and Conjecture 1:

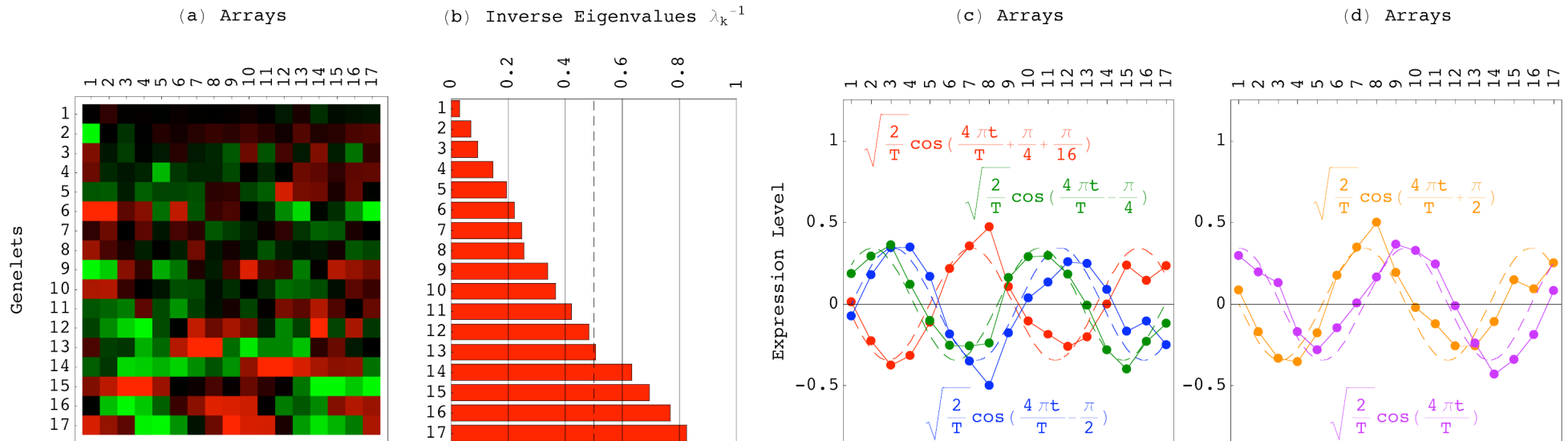
A role in iterative approximation algorithms.

Mathematical variables → biological reality

Genelets of almost equal significance in all datasets

→ processes common to all genomes:

Approximately Common HO GSVD Subspace



In a comparison of global cell cycle mRNA expression from *S. pombe*, *S. cerevisiae* and human, the approximately common HO GSVD subspace represents the cell cycle mRNA expression oscillations, which are similar among the datasets.

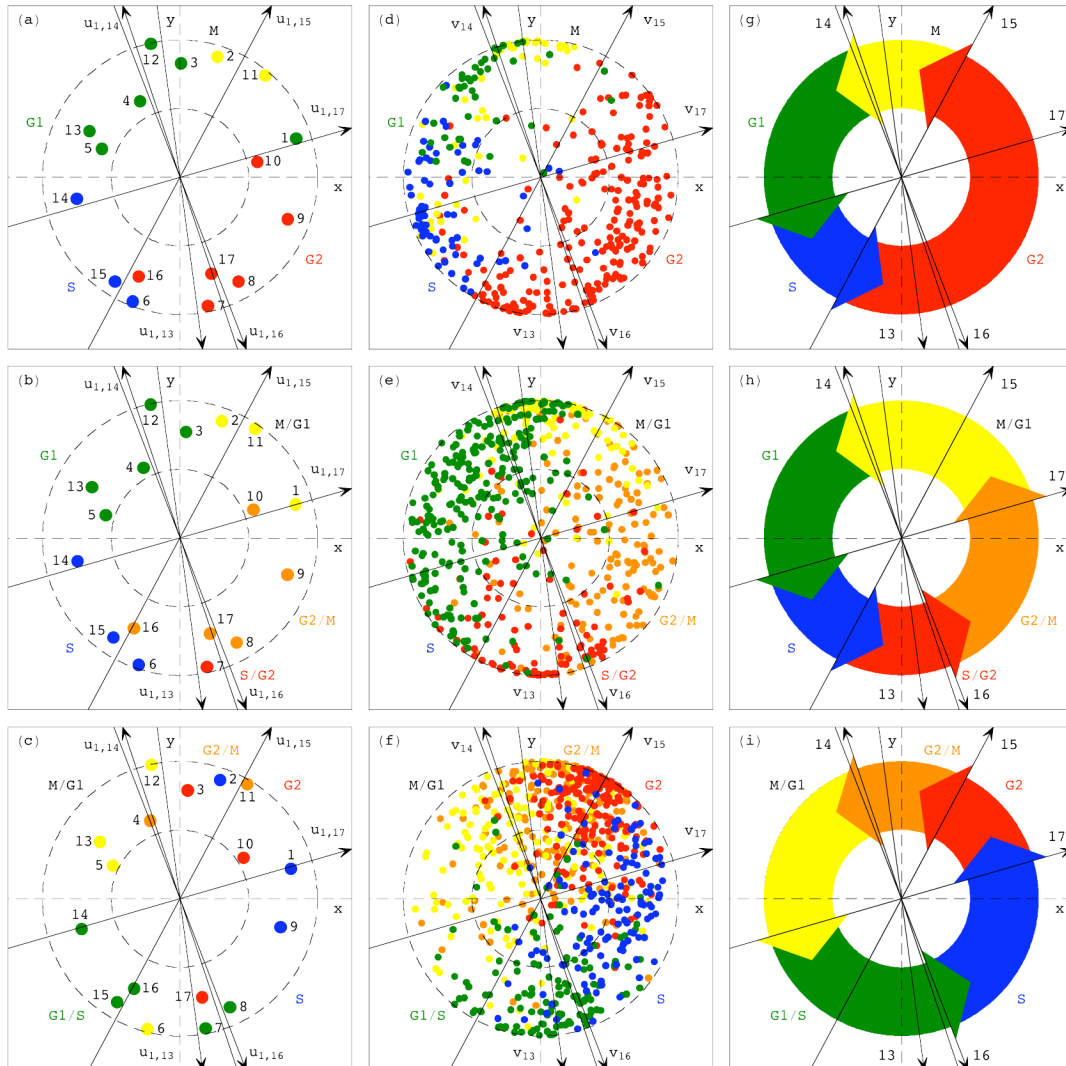
Simultaneous reconstruction in the common subspace, therefore, removes the experimental artifacts, which are dissimilar, from the datasets.

Mathematical operations → biological reality

Simultaneous classification in the common HO GSVD subspace

→ biological similarity in the regulation of the cellular programs that are conserved across the species:

Common Cell Cycle Subspace



Schizosaccharomyces pombe
Rustici et al., *Nat Genet* 36, 809 (2004).

Saccharomyces cerevisiae
Spellman et al., *MBC* 9, 3273 (1998).

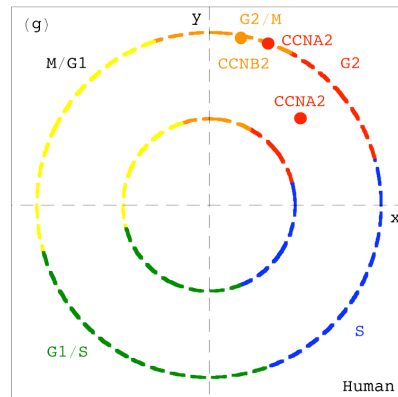
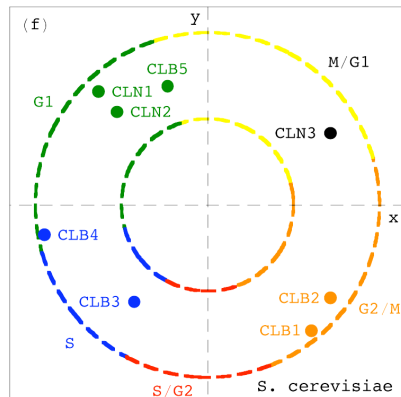
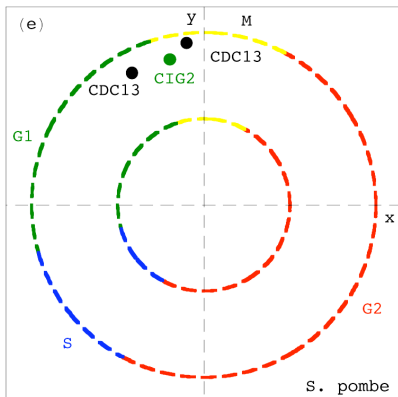
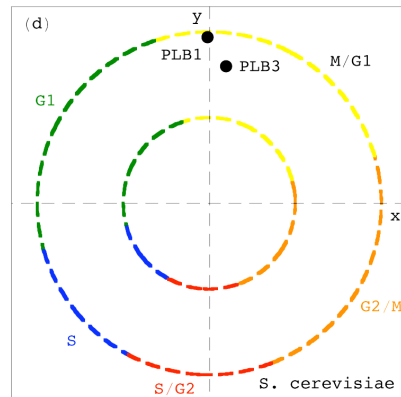
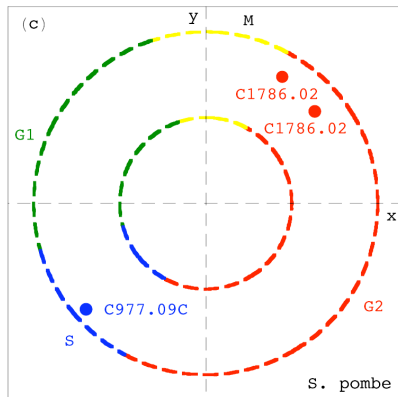
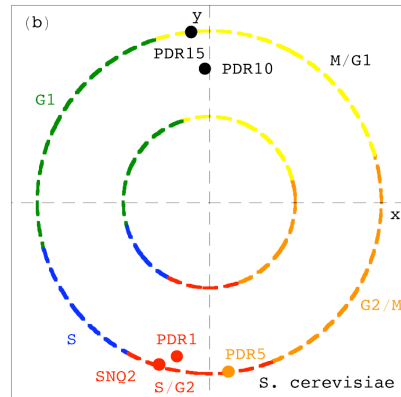
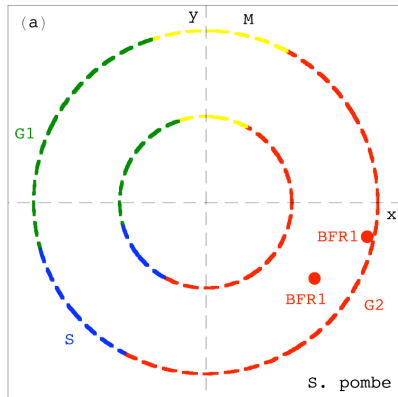
Human
Whitfield et al., *MBC* 13, 1977 (2002).

Simultaneous Classification Independent of Sequence Similarity

Genes of highly conserved sequences across the three organisms but significantly different cell cycle peak times are correctly classified.

ABC Transporter Superfamily Genes

Phospholipase B-Encoding Genes and
B Cyclin-Encoding Genes



Patterns Underlie Principles of Nature: Statistics to Processes

→ Brownian motion.

Einstein, *Ann Phys* 17, 549 (1905).

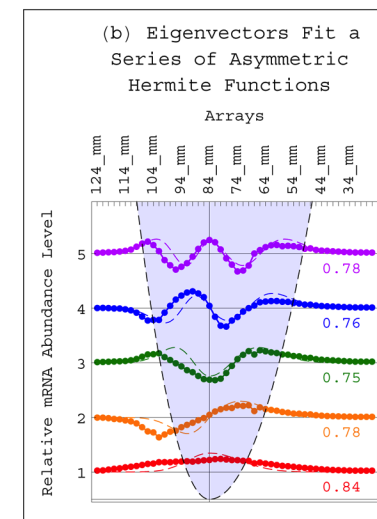
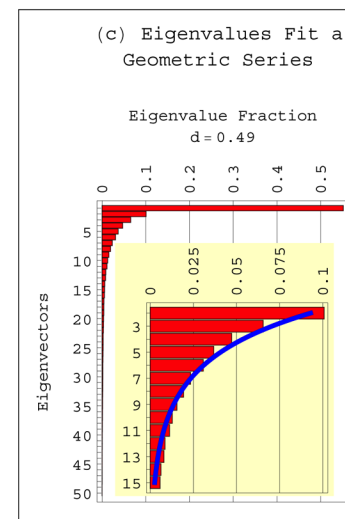
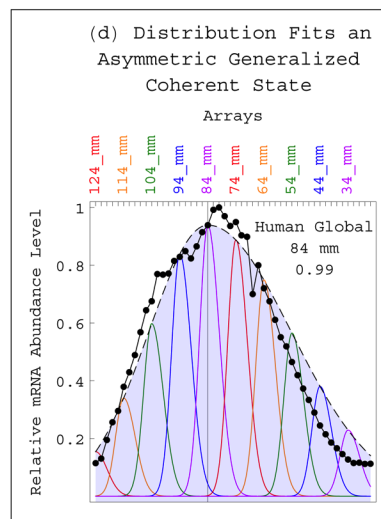
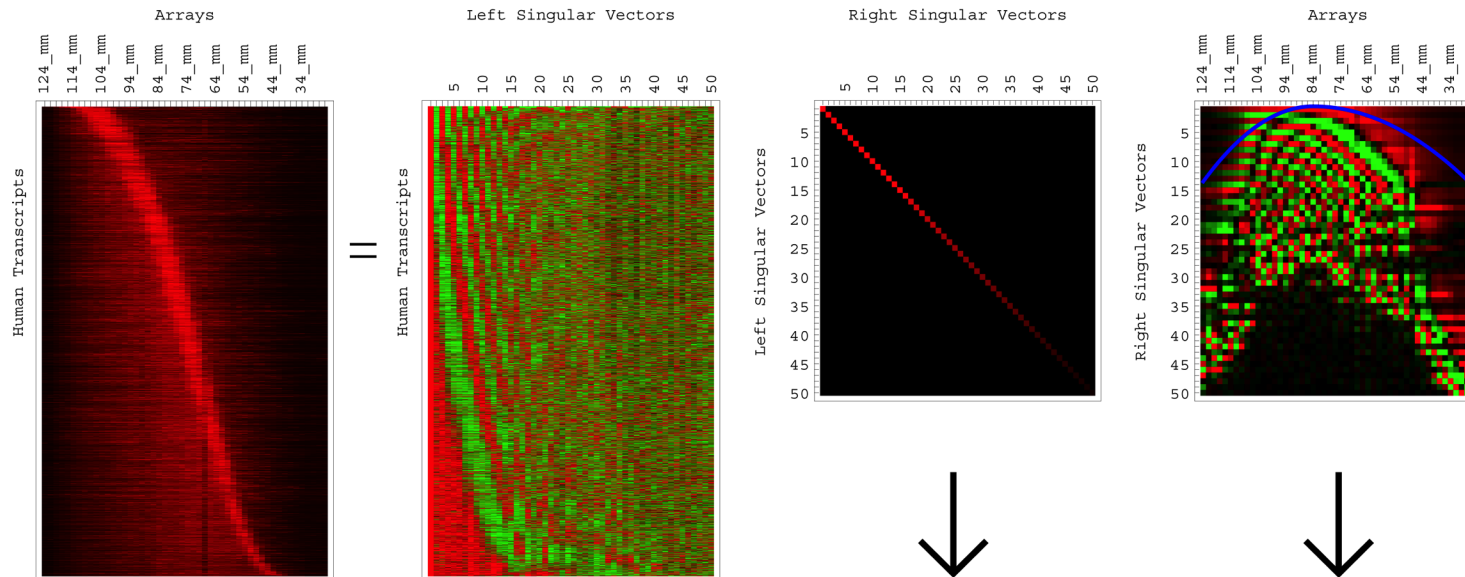
→ Bacterial sensitivity and resistance to viruses.

Luria & Delbrück, *Genetics* 28, 491 (1943).

SVD Identifies Transcript Length Distribution Functions from DNA Microarray Data

Bertagnoli, Drake, Tennessen & Alter, *PLoS One* 8, e78913 (2013);
http://alterlab.org/GBM_metabolism/

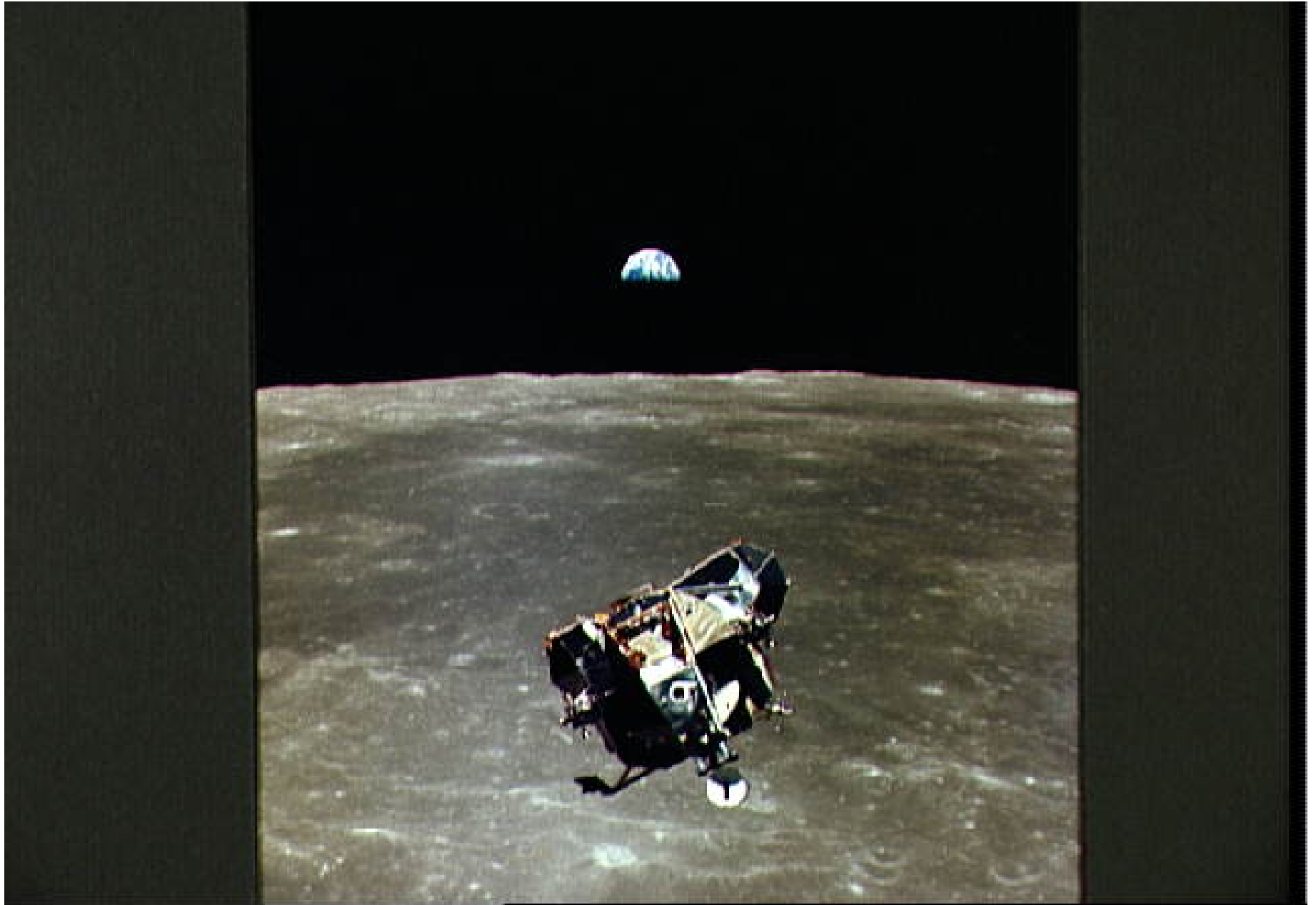
(a) Singular Value Decomposition Uncovers Left Singular Vectors, Singular Values and Right Singular Vectors



Alter & Golub, *PNAS* 103, 11828 (2006); http://alterlab.org/harmonic_oscillator/

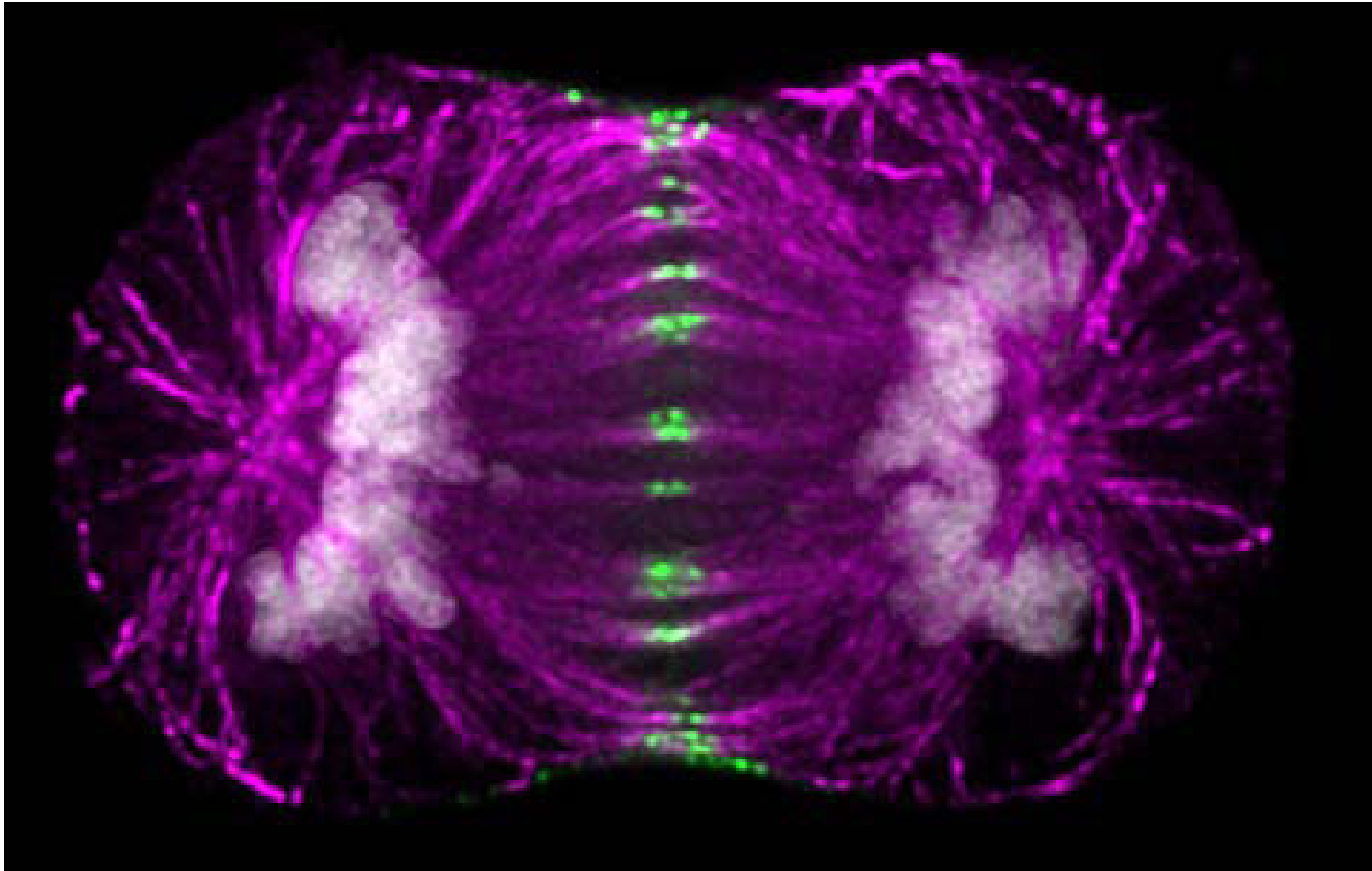
The interplay between mathematical modeling and experimental measurement is at the basis of the “effectiveness of mathematics” in physics.

Wigner, *Commun Pure Appl Math* 13, 1 (1960).



Mathematical modeling of large-scale molecular biological data can lead beyond classification of genes and cellular samples to the discovery and ultimately also control of molecular biological mechanisms.

Alter, *PNAS* 103, 16063 (2006).



Andrews & Swedlow, *Nikon Small World* (2002).

Our models bring physicians a step closer to one day being able to predict and control the progression of cancers as readily as NASA engineers plot the trajectories of spacecraft today.

Collaborators:

John F. X. Diffley

Cancer Research UK, London

Michael A. Saunders

Operations Research, Stanford

Charles F. Van Loan

Computer Science, Cornell

David Botstein

Genomics, Princeton

Patrick O. Brown

Biochemistry, Stanford

Gene H. Golub

Computer Science, Stanford

Support:

NHGRI K01 HG-000038

NHGRI R01 HG-004302

NSF CAREER DMS-0847173

NCI U01 CA-202144

Ph.D. Students:

Katherine A. Aiello, BE

Theodore E. Schomay, BE

K99 Postdoc Alumni:

Jason M. Tennessen, Genetics

Ph.D. Alumni:

Kayta Kobayashi, Pharmacy

Chaitanya Muralidhara, CMB

Larsson Omberg, Physics

Sri Priya Ponnappalli, ECE

Preethi Sankaranarayanan, BE

B.S. Alumni:

Nicolas M. Bertagnolli, Math

Justin A. Drake, BME & SSC

Andrew M. Gross, BME & SSC

Joel R. Meyerson, BME & Gov

Multi-Tensor Decompositions for Personalized Cancer Diagnostics and Prognostics

<http://physics.cancer.gov/network/UniversityofUtah.aspx>;
http://alterlab.org/physics_of_cancer/

Co-Investigators:

Elke A. Jarboe
Pathology, Utah

Randy L. Jensen
Neurosurgery, Utah

Cheryl A. Palmer
Pathology, Utah

Reha M. Toydemir
Pathology, Utah

Carl T. Wittwer
Pathology, Utah

Consultants:

Roger A. Horn
Mathematics, Utah

Ronald L. Weiss
Pathology, Utah

Orly Z. Ardon
Pathology, Utah

Thank you!!!

Physics-Inspired Multi-Tensor Decompositions

Create a single coherent model from multiple high-dimensional datasets. By using the complex structure of the datasets, rather than simplifying them as is commonly done, the frameworks can:

- detect and remove experimental artifacts or batch effects;
- identify and separate the biologically similar from the dissimilar;
- uncover previously unknown phenomena.

Generalize the SVD from a single two-dimensional dataset to multiple three- and higher-dimensional datasets. The SVD underlies:

- theoretical physics;
- recommendation systems, e.g., the Netflix challenge;
- Google's PageRank algorithm.

Find what others miss, and outperform algorithms that:

- are sensitive to artifacts (e.g., hierarchical clustering);
- require a-priori knowledge (e.g., analysis of variance);
- require data modifications (e.g., Bayesian statistics or topological data analysis);
- vary the single-dataset SVD (e.g., independent component analysis or randomized decompositions).

The SVD is also used for the stable computation of principal component analysis (PCA).

The SVD is Different than PCA

→ **PCA assumes preprocessing of the data, which limits the data interpretation** (e.g., the SVD of a dataset can identify the probability distribution function that is sampled by the dataset with no a-priori assumptions; PCA cannot).

Alter & Golub, *PNAS* 103, 11828 (2006);

Cadima & Jolliffe, *Pak J Statist* 25, 473 (2009);

Bertagnolli, Drake, Tennessen & Alter, *PLoS One* 8, e78913 (2013).

→ **PCA identifies patterns across the columns separately from patterns across the rows; the SVD simultaneously computes the corresponding sets of patterns across the rows and columns, ensuring consistent data interpretation.**

Alter, Brown & Botstein, *PNAS* 97, 10101 (2000);

Fellenberg, Hauser, Brors, Neutzner, Hoheisel & Vingron, *PNAS* 98, 10781 (2001).

→ **PCA, as it is programmed in most computational packages, is limited to classifying the data based upon the two or three patterns that capture most of the information in the data (e.g., variance in the case of column centering); the SVD maintains all data patterns, and not just for data classification.**